Atmos. Meas. Tech. Discuss., 8, 7573–7662, 2015
www.atmos-meas-tech-discuss.net/8/7573/2015/
doi:10.5194/amtd-8-7573-2015

Atmospheric Measurement Techniques Discussions

MIPAS IMK/IAA CFC-11 (CCl_3F) and CFC-12 (CCl_2F_2) measurements: accuracy, precision and long-term stability

E. Eckert[1], A. Laeng[1], S. Lossow[1], S. Kellmann[1], G. Stiller[1], T. von Clarmann[1], N. Glatthor[1], M. Höpfner[1], M. Kiefer[1], H. Oelhaf[1], J. Orphal[1], B. Funke[2], U. Grabowski[1], F. Haenel[1], A. Linden[1], G. Wetzel[1], W. Woiwode[1], P. F. Bernath[3], C. Boone[4], G. S. Dutton[5,6], J. W. Elkins[5], A. Engel[7], J. C. Gille[8,9], F. Kolonjari[10], T. Sugita[11], G. C. Toon[12], and K. A. Walker[4,10]

[1]Karlsruhe Institute of Technology, Institute of Meteorology and Climate Research, Karlsruhe, Germany
[2]Instituto de Astrofísica de Andalucía, CSIC, Granada, Spain
[3]Department of Chemistry and Biochemistry, Old Dominion University, Norfolk, VA 23529-0126, USA
[4]Department of Chemistry, University of Waterloo, Waterloo, Ontario, Canada
[5]NOAA Earth System Research Laboratory, Boulder, CO 80305, USA
[6]Cooperative Institute for Research in Environmental Sciences, University of Colorado, Boulder, CO 80309, USA
[7]Institut für Atmosphäre und Umwelt, J. W. Goethe Universität, Frankfurt, Germany

[8]National Center for Atmospheric Research, Boulder, Colorado, USA
[9]Center for Limb Atmospheric Sounding, University of Colorado, Boulder, Colorado, USA
[10]Department of Physics, University of Toronto, Toronto, Ontario, Canada
[11]National Institute for Environmental Studies, Tsukuba, Japan
[12]Jet Propulsion Laboratory, California Institute of Technology, Pasadena, CA 91109, USA

Received: 21 June 2015 – Accepted: 24 June 2015 – Published: 23 July 2015

Correspondence to: E. Eckert (ellen.eckert@kit.edu)

Published by Copernicus Publications on behalf of the European Geosciences Union.

AMTD
8, 7573–7662, 2015

Abstract

Profiles of CFC-11 (CCl_3F) and CFC-12 (CCl_2F_2) of the Michelson Interferometer for Passive Atmospheric Sounding (MIPAS) abord the European satellite Envisat have been retrieved from versions MIPAS/4.61–MIPAS/4.62 and MIPAS/5.02–MIPAS/5.06 level-1b data using the scientific level-2 processor run by Karlsruhe Institute of Technology (KIT), Institute of Meteorology and Climate Research (IMK) and Consejo Superior de Investigaciones Científicas (CSIC), Instituto de Astrofísica de Andalucía (IAA). These profiles have been compared to measurements taken by the balloon borne Cryosampler, Mark IV (MkIV) and MIPAS-Balloon (MIPAS-B), the airborne MIPAS stratospheric aircraft (MIPAS-STR), the satellite borne Atmospheric Chemistry Experiment Fourier transform spectrometer (ACE-FTS) and the High Resolution Dynamic Limb Sounder (HIRDLS) as well as the ground based Halocarbon and other Atmospheric Trace Species (HATS) network for the reduced spectral resolution period (RR: January 2005–April 2012) of MIPAS Envisat. ACE-FTS, MkIV and HATS also provide measurements during the high spectral resolution period (FR: July 2002–March 2004) and were used to validate MIPAS Envisat CFC-11 and CFC-12 products during that time, as well as ILAS-II profiles. In general, we find that MIPAS Envisat shows slightly higher values for CFC-11 at the lower end of the profiles (below ~ 15 km) and in a comparison of HATS ground-based data and MIPAS Envisat measurements at 3 km below the tropopause. Differences range from approximately 10–50 pptv (~ 5–20 %) during the RR period. In general, differences are slightly smaller for the FR period. An indication of a slight high-bias at the lower end of the profile exists for CFC-12 as well, but this bias is far less pronounced than for CFC-11, so that differences at the lower end of the profile (below ~ 15 km) and in the comparison of HATS and MIPAS Envisat measurements taken at 3 km below the tropopause mainly stay within 10–50 pptv (~ 2–10 %) for the RR and the FR period. Above approximately 15 km, most comparisons are close to excellent, apart from ILAS-II, which shows large differences above ~ 17 km. Overall, percentage differences are usually smaller for CFC-12 than for CFC-11. For both

AMTD
8, 7573–7662, 2015

species – CFC-11 and CFC-12 – we find that differences at the lower end of the profile tend to be larger at higher latitudes than in tropical and subtropical regions. In addition, MIPAS Envisat profiles have a maximum in the mixing ratio around the tropopause, which is most obvious in tropical mean profiles. Estimated measurement noise alone can, in most cases, not explain the standard deviation of the differences. This is attributed to error components not considered in the error estimate and also to natural variability which always plays a role when the compared instruments do not measure exactly the same air mass. Investigations concerning the temporal stability show very small negative drifts in MIPAS Envisat CFC-11 measurements. These drifts vary between ~ 1–3 % decade^{-1}. For CFC-12, the drifts are also negative and close to zero up to ~ 30 km. Above that altitude larger drifts of up to ~ 50 % decade^{-1} appear which are negative up to ~ 35 km and positive, but of a similar magnitude, above.

1 Introduction

Chlorofluorocarbons (CFCs) have been monitored for some decades, because of their potential to release catalytically active species that destroy stratospheric ozone, which was first discovered by Molina and Rowland (1974). Even though there are also natural sources of halogens, observations focus on man-made CFCs such as CFC-11 and CFC-12, because increased release of active chlorine species due to elevated amounts of these substances can significantly alter the equilibrium of stratospheric ozone formation and destruction. Under certain conditions (sufficiently cold temperatures for chlorine activation; polar stratospheric clouds, PSCs) this can lead to severe ozone depletion. The consequential outcome of the combination of elevated amounts of active chlorine species – due to increased CFC emissions in the past – with chlorine activation under cold temperatures and PSCs can be observed in the Antarctic each winter – and, occasionally, even in the Arctic during some winters – in severe ozone depletion and the formation of the Antarctic ozone hole. Since CFCs have very long lifetimes in the atmosphere (50 ± 5 years for CFC-11; 102 years for CFC-12 (Brasseur

AMTD
8, 7573–7662, 2015

and Solomon, 2005), also comp. SPARC Report No. 6, 2013) and are insoluble in water, they can easily reach the stratosphere, because they are neither destroyed nor washed out before they arrive at middle atmospheric regions. In the stratosphere, halogen source gases, such as CFC-11 or CFC-12, are photolysed or otherwise broken up and finally converted to so-called reservoir gases, particularly hydrogen chloride (HCl) or chlorine nitrate ($ClONO_2$), by chemical reactions and under the influence of solar ultraviolet radiation. Stratospheric abundances of hydrogen chloride and chlorine nitrate increased significantly during the later decades of the past century (World Meteorological Organization, 2011), as a consequence of intensified anthropogenic emissions of CFCs and other ozone depleting substances (ODSs), which were used for refrigeration, foam blowing and several other purposes. While direct reactions of ozone with the reservoir species HCl and $ClONO_2$ are not relevant for ozone depletion, these reservoir species are transformed into active chlorine species (ClO_x; mainly ClO and Cl_2O_2) under sufficiently cold temperatures. The active chlorine species catalytically destroy ozone via the so-called ClO-dimer cycle (Molina and Molina, 1987) and the synergistic interaction of ClO and BrO (McElroy et al., 1986). Here, heterogeneous reactions on the surfaces of cold aerosol of PSCs occur and, in combination with sunlight, result in the reactivation of chlorine which can then destroy ozone catalytically and ultimately leads to ozone depletion and the formation of the ozone hole.

Once it was observed (Farman et al., 1985) that these processes could lead to severe ozone depletion in reality, the Montreal Protocol was adopted in 1987 to control the emission of CFCs and other ozone depleting substances. Afterwards, the emission of CFCs decreased and ceased completely in 2010 (World Meteorological Organization, 2011), which led to decreasing amounts of these species in the atmosphere. However, since several CFCs have lifetimes of up to a hundred years and more – which makes them excellent tracers for the Brewer-Dobson circulation (Schoeberl et al., 2005; SPARC Report No. 6, 2013) – significant amounts of these species are still present in the atmosphere. Hence, their monitoring and the closer examination of their evolution in the atmosphere are important tasks, as Kellmann et al. (2012) have shown by illus-

AMTD
8, 7573–7662, 2015

trating that there are trends in CFC-11 and CFC-12 which can so far only be explained by changes in circulation.

In addition to their ozone depleting potential, CFC-11 and CFC-12 have a pronounced global warming potential (comp. World Meteorological Organization , WMO, e.g. Fig. 1-6-4), which is another reason for monitoring these species. In the following, we describe the data products and the different characteristics of the instruments used in the comparisons (Sect. 2), followed by an explanation of the validation method (Sect. 3). Since MIPAS Envisat malfunctioned in 2004 and the retrieval setup had to be changed afterwards to address the altered situation, two sets of the data exist for either species, one (FR = full spectral resolution) referring to the period of July 2002 to March 2004 and one (RR = reduced spectral resolution) referring to the period of January 2005–April 2012. The spectral resolution deteriorated from the FR to the RR period, but more scans in the vertical are performed per profile during the RR period (comp. Kellmann et al., 2012, Table 1). Thus, in Sect. 4 we show the extensive results of the validation of version V5R_220 and V5R_221 (corresponding to the RR period) of MIPAS Envisat CFC-11 and CFC-12 products and also a few comparisons for version V5H_20 (corresponding to the FR period) of the same species. A concluding summary is closing the paper.

2 Instruments

2.1 MIPAS Envisat data and retrieval

The Michelson Interferometer for Passive Atmospheric Sounding (MIPAS) was one of 10 instruments aboard Envisat (Environmental Satellite). The satellite was launched into a polar, sun-synchronous orbit on 1 March 2002 from the Guyana Space Centre in Kourou (French Guyana). The last contact with the satellite was made on 8 April 2012. This adds up to an observation period of 10 years. Envisat orbited the Earth

AMTD
8, 7573–7662, 2015

14 times a day at an altitude of 790 km. The equator crossing times were 10 local time and 22 local time for the descending and ascending node, respectively.

The MIPAS Envisat instrument was a high-resolution Fourier transform spectrometer. It measured thermal emission at the atmospheric limb in the mid-infrared range between 685 and 2410 cm^{-1} (4.1 and 14.6 µm) (Fischer et al., 2008). The MIPAS Envisat measurement period is split into two parts based on the spectral resolution of the measurements. Until March 2004 the measurements were performed with a spectral resolution of 0.035 cm^{-1} (unapodized), which was the nominal setting. Due to an instrumental failure later measurements, commencing in January 2005, could only be performed with a reduced resolution of 0.0625 cm^{-1}. In correspondence we denote the two periods as full (FR) and reduced (RR) spectral resolution periods, respectively. In the present validation study we focus on measurements that were performed in the "nominal observation mode". In this mode spectra at 17 tangent heights between 6 and 68 km were obtained in the FR period. The horizontal sampling was about 1 scan per 510 km and overall more than 1000 scans were performed per day. During the RR period the sampling improved in the horizontal domain to 1 scan per 410 km and in the vertical domain to 27 spectra between 7 and 72 km. More than 1300 scans were obtained on a single day covering the entire latitude range.

The CFC-11 and CFC-12 data sets that are used in this study have been retrieved with the IMK/IAA processor that has been set up together by the Institute of Meteorology and Climate Research (IMK) in Karlsruhe (Germany) and the "Instituto de Astrofísica de Andalucía" (IAA) in Granada (Spain). The retrieval employs a non-linear least squares approach with a first-order Tikhonov-type regularisation (von Clarmann et al., 2003, 2009). The simulation of the radiative transfer through the atmosphere is performed by the KOPRA (Karlsruhe Optimized and Precise Radiative Transfer Algorithm) model (Stiller, 2000). In the comparisons we consider data that was retrieved with the retrieval versions V5H_CFC-11_20 and V5H_CFC-12_20 for the FR period as well as V5R_CFC-11_220/221 and V5R_CFC-12_220/221 for the RR period (Kellmann et al., 2012). Version 220 covers the time period from January 2005 to April 2011 and

AMTD
8, 7573–7662, 2015

version 221 is attributed to the time afterwards. The only change between these two versions is the source of the temperature a priori data. Initially the a priori data were based on NILU's (Norwegian Institute of Air Research) post-processing of ECMWF (European Centre for Medium-Range Weather Forecasts) data. Later they were taken from ECMWF directly as NILU's processing had ceased. CFC-11 data is derived from spectral information in the wavelength range between 831 and 853 cm^{-1} (11.72 and 12.03 µm). Information on the vertical distribution of CFC-11 can be obtained in the altitude range of 5 and 30 km with a single profile precision within 5 % below 20 km and 40 % at the upper limit. The altitude resolution is 3 up to 20 km and about 7 at 30 km altitude for the FR period and somewhat better, typically by 1 km, for the RR period. The CFC-12 retrieval uses spectral information between 915 and 925 cm^{-1} (10.69 and 10.93 µm) providing coverage from 5 km to somewhat above 40 km. The single profile precision is very similar to that of CFC-11, with slightly worse values at the uppermost altitude limit. The vertical resolution of the retrieved FR data is typically within 3–4 up to 25 km and decreases to 6–8 km at altitudes above 40 km. As for CFC-11, the RR data has a slightly better vertical resolution. Overall, the CFC data sets comprise more than 480000 individual profiles for the FR period and more than 1.8 million profiles for the RR period.

2.2 Comparison instruments

2.2.1 Cryosampler data

The Cryosampler instrument is a balloon-borne cryogenic whole air sampler originally developed at Forschungszentrum Jülich (Germany) in the early 1980s (Schmidt et al., 1987). The cryosampler used in this comparison is the BONBON instrument. The first observations date back to 1982. The instrument consists of a dewar with 15 stainless steel sampling containers which is filled with liquid neon to cool the sampling containers down to 27 K. This allows the sampling of a sufficient mass of air even at low pressures, which will freeze out immediately. The sampling is controlled via a telecommand that

AMTD
8, 7573–7662, 2015

initiates the opening and closing of the sampler inlets. An inlet is opened by breaking a glass cap that seals it off. A gold pipe in the inlet is welded by a pyrotechnical device to close the inlet and stop the sampling. The sampler inlets face downward, hence the BONBON measurements are optimized for the descending leg of the flight in order to avoid contamination from balloon outgassing. After the flight the collected samples are analyzed on the abundance of a long list of trace gases by means of gas chromatography. In the comparison we consider five balloon flights that were operated by the University of Frankfurt (Germany) (e.g. Laube et al., 2008).

2.2.2 MkIV data

The Mark IV interferometer is a balloon-borne high-resolution Fourier transform spectrometer which has been developed at the Jet Propulsion Laboratory in Pasadena (USA) in the 1980s. The instrument employs the solar occultation technique measuring absorption spectra over a wide wavelength range from 650–5650 cm^{-1} (1.77–15.39 µm) with a very high spectral resolution of up to 0.006 cm^{-1}. It had its inaugural flight in 1989 and since then more than 20 flights were conducted (Toon, 1991; Velazco et al., 2011). The flight duration varies between a few hours up to 30 h allowing one or two occultations to be taken during one flight. The occultations cover the altitude range between the tropospheric cloud tops and the floating altitude which is typically within the 35–40 km range. The vertical sampling is about 2–4 km. The profile retrieval is based on an iterative non-linear least square fitting algorithm with a derivative constraint. CFC-11 information is retrieved from a single microwindow between 830.75–861.65 cm^{-1} (11.60 and 12.04 µm). The CFC-12 retrieval uses spectral information from two microwindows. A broader one ranges from 920.0–923.6 cm^{-1} (12.83–12.87 µm) and a smaller one is located between 1160.25–1161.75 cm^{-1} (8.61–8.62 µm). The vertical resolution of the retrieved data is close to the vertical sampling.

AMTD
8, 7573–7662, 2015

2.2.3 MIPAS-B data

MIPAS-B denotes a balloon-borne version of the MIPAS type of instruments and can be regarded as a precursor of the satellite instrument that flew on Envisat as described in Sect. 2.1. The instrument was developed in the late 1980s and early 1990s at the "Institut für Meteorologie und Klimaforschung" in Karlsruhe (Germany) and two models were built (Fischer and Oelhaf, 1996; Friedl-Vallon et al., 2004). The maiden flight was conducted in 1989 (von Clarmann et al., 1993) and since then more than 20 flights were carried out. The spectral coverage and resolution of MIPAS-B is equivalent to the satellite version. Balloon-borne observations require excellent pointing accuracy that is realized by a sophisticated line of sight stabilization system. Also multiple spectra taken at the same elevation angle are averaged up to reduce the noise of the measurement data for the comparison with MIPAS Envisat. Typically the MIPAS-B floating altitude lies between 30 and 40 km and limb scans are performed with a vertical sampling of about 1.5 km up to this altitude. The retrieval algorithm for MIPAS-B observations is based on the same retrieval strategy and forward model as that employed by the MIPAS Envisat IMK/IAA processor, however the microwindows from which the CFC information is derived are slightly different. For the CFC-11 retrieval spectral information in the wavelength range between 840.0–860.0 cm^{-1} (11.63 and 11.90 µm) is used, while the CFC-12 retrieval utilizes spectral information between 918.0–924.0 cm^{-1} (10.82 and 10.89 µm) (Wetzel et al., 2013). The retrieved profiles typically have a vertical resolution in the order of 2–5 km. In total eight balloon flights were performed during the life time of MIPAS Envisat. Five of these flights were conducted during the reduced resolution period from 2005 to 2012 which is the key period of the present comparisons.

2.2.4 MIPAS-STR data

The cryogenic Fourier transform infrared limb-sounder Michelson Interferometer for Passive Atmospheric Sounding – STRatospheric aircraft (MIPAS-STR; Piesch et al., 1996) aboard the high-altitude research aircraft M55 Geophysica is the airborne sister

AMTD
8, 7573–7662, 2015

instrument of MIPAS. Here we use MIPAS-STR observations during the Arctic RECONCILE campaign (Reconciliation of essential process parameters for an enhanced predictability of Arctic stratospheric ozone loss and its climate interactions; von Hobe et al., 2013) for the validation of MIPAS Envisat observations. The characterization, calibration, L1-processing, retrieval and validation of the MIPAS-STR observations during the considered flight on 2 March 2010 are discussed by Woiwode et al. (2012). Characteristics of MIPAS-STR, the data processing and uncertainties of the retrieval results are briefly summarized in the following. Further information on MIPAS-STR is found in Keim et al. (2008); Woiwode et al. (2014) and references therein.

MIPAS-STR employs four liquid He-cooled detectors/channels in the spectral range between 725 and 2100 cm^{-1} (4.8 and 13.8 µm). The spectral sampling is 0.036 cm^{-1}. An effective spectral resolution of 0.069 cm^{-1} (full width at half maximum) is obtained after applying the Norton-Beer strong apodization (Norton and Beer, 1976). For the retrieval of CFC-11 and CFC-12, MIPAS-STR channel 1 spectra (725–990 cm^{-1}, 10.1–13.8 µm) with a noise-equivalent spectral radiance (NESR) of $\sim 10 \times 10^{-9}$ W cm^{-2} sr^{-1} cm are used. Depending on the sampling program, the dense MIPAS-STR limb-observations cover the vertical range between ~ 5 km and flight altitude (in Arctic winter typically at 17–19 km geometrical altitude) and are complemented by upward-viewing observations. A complete limb-scan including calibration measurements is recorded typically within 2.4–3.8 min. This corresponds to an along-track sampling of about 25–45 km.

For the retrieval of CFC-11, the spectral microwindow from 842.5–848.0 cm^{-1} (11.87–11.79 µm) was utilized. CFC-12 was retrieved using the combination of the spectral microwindows from 918.9 to 920.6 cm^{-1} (10.86–10.88 µm) and from 921.0 to 922.8 cm^{-1} (10.84–10.86 µm). Similar to the MIPAS Envisat data processing, the forward model KOPRA (Karlsruhe Optimized and Precise Radiative Transfer Algorithm; Stiller, 2000) and the inversion module KOPRAFIT (Höpfner et al., 2001), involving a first-order Tikhonov-type regularization, were used. The retrieval was performed sequentially, i.e. species with low spectral interference with other gases were retrieved

AMTD
8, 7573–7662, 2015

first. Then, their mixing ratios were kept constant in the subsequent retrievals of the following species. Additional retrieval parameters were spectral shift and wavenumber-independent background continuum for each microwindow. The shown 1σ error of the MIPAS-STR retrieval results consists of the spectral noise error. Typical vertical resolutions of 1–2 km were obtained between the lowest tangent altitude and flight altitude.

2.2.5 Aura/HIRDLS data

The High Resolution Dynamics Limb Sounder (HIRDLS) was an instrument that performed observations aboard NASA's (National Aeronautics and Space Administration) Aura satellite (Gille et al., 2008). On 15 July 2004 the satellite was launched from Vandenburg Air Force Base into a sun-synchronous orbit at an altitude of 705 km. During launch large parts (~ 85 %) of the instrument's aperture got blocked by a plastic film that was dislocated. This impacted both the performance of the radiometer as well as the geographical coverage of the observations. Useful vertical scans could only be performed at a single azimuth angle of 47° backward to the orbital plane on the far side of the sun. Hence, the latitudinal coverage was limited to 65° S–82° N and in the longitudinal domain the coverage degraded to the orbital separation. On 17 March 2008 the instrument's chopper failed, ending the measurement period that started in January 2005.

Like MIPAS Envisat, HIRDLS measured the thermal emission at the atmospheric limb in the altitude range between 8 and 80 km. The instrument had 21 channels in the wavelength range between 6.12 and 17.64 µm (566.9 and 1632.9 cm^{-1}). Data from channel no. 7 (11.75–11.99 µm/834–851 cm^{-1}) is used for the CFC-11 retrieval; channel no. 9 (10.73–10.93 µm/915–932 cm^{-1}) provides the spectral information for the CFC-12 retrieval. Profile data are retrieved with a maximum a posteriori retrieval based on the optimal estimation theory (Rodgers, 2000). In the present comparison data from the retrieval version 7 are used (Gille et al., 2014). Valid data for CFC-11 can be retrieved within the altitude range of 316 and 17.8 hPa. For CFC-12 the range extends up to 8.3 hPa. The single profile precision for both species minimizes between 200 and

AMTD
8, 7573–7662, 2015

100 hPa with values in the range between 10 and 20 %. Below, the precision is within the order of 50 % while above it degrades with increasing altitude to values of more than 100 %. The vertical resolution is approximately 1.0–1.2 km for both species. The mean HIRDLS errors shown in the comparisons are derived from the variability of the retrieved species (comp. Gille et al., 2014, Sects. 5 and 5.4.) using the average of 10 sets of 12 consecutive profiles of regions with little variability. In total the HIRDLS data set comprises more than 6.3 million individual profiles that can be used for comparison with the MIPAS Envisat reduced resolution observations.

2.2.6 SCISAT/ACE-FTS data

The Atmospheric Chemistry Experiment Fourier Transform Spectrometer (ACE-FTS) is an instrument aboard the Canadian SCISAT satellite (Bernath et al., 2005). SCISAT was launched into a high inclination (74°) orbit at 650 km altitude on 12 August 2003 from Vandenburg Air Force Base in California (USA). The ACE-FTS instrument utilizes the solar occultation technique measuring the attenuation of sunlight by the atmosphere during 15 sunsets and 15 sunrises a day in two latitude bands. The viewing geometry and the satellite orbit allow a latitudinal coverage between 85° S and 85° N over a year with a clear focus on mid and high latitudes. The instrument scans the atmosphere between the middle troposphere and 150 km obtaining spectra in the wavelength range between 2.3 and 13.3 µm (750 and 4400 cm^{-1}) with a spectral resolution of 0.02 cm^{-1}. The vertical sampling varies as function of altitude and is also dependent on the beta angle, which is the angle between the orbit track and the direction the instrument has to look to see the sun. In the middle troposphere the sampling is around 1 km, between 10 and 20 km altitude it is typically between 2 and 3.5 km and in the upper stratosphere and mesosphere the sampling declines to 5–6 km. The instrument has a field of view of 1.25 mrad which corresponds to 3–4 km depending on the exact observation geometry.

In the comparisons ACE-FTS data from the retrieval version 3.5 are employed, which currently cover the time period from early 2004 into 2013. The ACE-FTS retrieval uses

AMTD
8, 7573–7662, 2015

a weighted non-linear least squares fit method in which pressure and temperature profiles are derived in a first step followed by the volume mixing ratios of a vast number of species (Boone et al., 2005). The retrieval of CFC-11 data utilizes spectral information from 4 microwindows. The main window is located between 11.65 and 12.05 µm (830 and 858 cm^{-1}), similar to the MIPAS Envisat IMK/IAA retrieval. The other microwindows are much smaller and are centred at 3.35 µm (2976.5 cm^{-1}), 5.06 µm (1977.6 cm^{-1}) and 5.08 µm (1970.1 cm^{-1}). However, these microwindows do not contain information on CFC-11 but are included to improve the retrieval for interfering species (Boone et al., 2013). The retrieved profiles cover altitudes from 6 km to about 25–30 km. Individual profiles exhibit precisions within 5 % up to almost 20 km increasing to 40–50 % at the highest altitudes covered. A microwindow between 10.82 and 10.87 µm (920 and 923.8 cm^{-1}) is used to infer CFC-12 data from the ACE-FTS measurements. The ACE-FTS CFC-12 profiles are usually cut off at higher altitudes than the CFC-11 profiles, but exhibit similar precision estimates. The cut-off criteria for CFC-11 and CFC-12 are empirical functions as follows:

– For CFC-11:

$$z_{\text{top, CFC-11}} = 28 - 5 \cdot \sin^2(\varphi) \quad (1)$$

– For CFC-12:

$$z_{\text{top, CFC-12}} = 36 - 8 \cdot \sqrt{\sin(\varphi)} \quad (2)$$

where $z_{\text{top, CFC-11}}$ and $z_{\text{top, CFC-12}}$ are the altitude (in kilometers) at which the profile is cut off for CFC-11 and CFC-12, respectively, and φ is the latitude. The vertical resolution of the data ranges between 3 and 4 km and is associated with the field of view. Overall, there are about 27000 CFC-11 and CFC-12 profiles available for comparison, of which 375 cover the MIPAS Envisat FR period.

AMTD
8, 7573–7662, 2015

2.2.7 ADEOS-II/ILAS-II

The second edition of the Improved Limb Atmospheric Spectrometer (ILAS-II) was a Japanese solar occultation instrument aboard the Advanced Earth Observing Satellite-II (ADEOS-II), also known as Midori-II Nakajima et al. (2006). The satellite was launched on 14 December 2002 from Tanegashima Space Center which is located on an island south of Kyushu. After more than 10 months, on 24 October 2003, the satellite failed due to a malfunction of the solar panels. ADEOS-II used a sun-synchronous orbit at 800 km altitude and an inclination of 98.7°, performing typically 14 orbits per day. The corresponding 28 occultations covered exclusively higher latitudes, i.e. polewards of 64° in the Southern Hemisphere and between 54 and 71° in the northern counterpart. The instrument consisted of four grating spectrometers obtaining spectral information in the infrared (spectrometer 1: 6.21–11.76 µm/850–1610 cm^{-1}; spectrometer 2: 3.00–5.70 µm/1754–3333 cm^{-1}; spectrometer 3: 12.78–12.85 µm/778–782 cm^{-1}) and very close to the visible wavelength range (spectrometer 4: 753–784 nm/12 755–13 280 cm^{-1}). The spectral resolution was 0.129 µm for spectrometer 1 and 2, 0.0032 µm for spectrometer 3 and 0.15 nm for spectrometer 4, respectively. The instantaneous field of view was 1 km in vertical domain and between 2 and 21.7 km in the horizontal domain, depending on spectrometer.

In the comparisons we employ results from the latest retrieval version 3. The retrieval is based on an onion peeling method Yokota et al. (2002). Multiple parameters for gases and aerosols are derived simultaneously on a 1 km altitude grid using a least squares fit (Oshchepkov et al., 2006). In this version 3, the HITRAN 2004 database (Rothman et al., 2005) is used for the molecular spectroscopic data in the infrared. The CFC results are based on the spectrum obtained by spectrometer 1 that is fitted in its entirety. The CFC-11 data typically cover the altitude range between 10 and 30 km. For the CFC-12 data the lower limit is the same, however they extend higher up to about 35 km. The vertical resolution at the lower limit is better than 1.5 km and decreases to about 2.5 km at the upper boundary. For the comparisons with MIPAS Envisat more

AMTD
8, 7573–7662, 2015

than 5600 individual profiles are available covering the time period from April–October 2003 Nakajima et al. (2006) and thus provide comparison measurement for the MIPAS Envisat FR period. For sunrise measurement, only measurements below 34 km were considered as suggested by the data provider.

2.2.8 HATS data

HATS denotes the Halocarbons and other Atmospheric Trace Species group at NOAA's (National Oceanic and Atmospheric Administration) Earth System Research Laboratory in Boulder (USA). Since 1977 this group conducts observations of surface levels of N_2O and several CFCs providing a long-term reference (e.g. Elkins et al., 1993; Montzka et al., 1996). These measurements are analyzed by gas chromatography either with electron capture detection or with detection by mass spectrometry. The observations started at six locations, currently 15 locations are covered on all continents except Asia. Data from different measurement techniques and instruments are combined to provide the longest possible monthly mean time series for the individual locations. In the comparison we check if the tropospheric MIPAS Envisat observations exceed the upper volume mixing ratio limit that is given by the HATS observations and if their temporal development is consistent.

HATS data are available for more than a dozen stations during the MIPAS Envisat measurement period. Their measurements were weighted with the cosine of latitude and an average was calculated for each day.

3 Validation methods

In order to reduce the influence of natural variability and sampling artefacts, the majority of the comparisons were performed using collocated pairs of measurements. During this study, the coincidence criteria applied in most of the cases were a maximum distance of 1000 km and maximum time difference of 24 h. In the case of HIRDLS

AMTD
8, 7573–7662, 2015

the criteria were cut down to a distance of 250 km and a time difference of 6 h, due to the large number of measurements of the instrument. No measurement is taken into account twice, meaning that only the best coincidence is taken in cases where two measurements of one instrument collocate with the same measurement of the other instrument. For MIPAS-B comparisons, diabatic 2 day forward and backward trajectories were calculated by the Free University of Berlin (J. Abalichin, private communication, 2014). The trajectories are based on ECMWF 1.25° × 1.25° analyses and start at different altitudes at the geolocation of the balloon observation to search for a coincidence with the satellite measurement along the trajectory path within a matching radius of 1 h and 500 km. Data of the satellite match have been interpolated onto the trajectory match altitude such that these values can be directly compared to the MIPAS-B data at the trajectory start point. The MIPAS Envisat averaging kernels were not applied in any of the comparisons, due to two reasons: first of all, most of the instruments used for comparison have a vertical resolution similar to that of MIPAS Envisat. In addition, the vertical profiles of CFC-11 and CFC-12 are very smooth and rather flat. They do not contain any obvious extrema – as for example ozone does – and thus smoothing with the MIPAS Envisat averaging kernel was shown to have only minor effects on the profiles. Comparison instrument measurements were interpolated onto the MIPAS Envisat grid, which is a fixed altitude grid with one kilometer spacing in the altitude range relevant for comparison of CFC-11 and CFC-12. When provided on an altitude grid the instruments measurements were interpolated linearly onto the MIPAS Envisat grid, while in the case of a pressure grid the MIPAS Envisat pressure-altitude relation was used after logarithmic interpolation.

For the comparison of MIPAS-STR, HIRDLS, ACE-FTS and ILAS-II, the mean difference of n contributing profiles pairs of the MIPAS Envisat measurement ($x_{i,\mathrm{MIPAS}}$) and the comparison instrument measurement ($x_{i,\mathrm{comp}}$)

$$\mathrm{MD} = \frac{1}{n}\sum_{i=1}^{n}\left(x_{i,\mathrm{MIPAS}} - x_{i,\mathrm{comp}}\right) \quad (3)$$

AMTD
8, 7573–7662, 2015

– including the standard error of the mean –

$$\sigma_{\overline{\Delta x}} = \frac{\sqrt{\frac{1}{n-1}\sum_{i=1}^{n}\left(\left(x_{i,\mathrm{MIPAS}} - x_{i,\mathrm{comp}}\right) - \mathrm{MD}\right)^2}}{\sqrt{n}} \quad (4)$$

was assessed and the standard deviation of the differences

$$\sigma_{\Delta x} = \sqrt{\frac{1}{n-1}\sum_{i=1}^{n}\left(\left(x_{i,\mathrm{MIPAS}} - x_{i,\mathrm{comp}}\right) - \mathrm{MD}\right)^2} \quad (5)$$

and the combined error of the measurements

$$\sigma_{\mathrm{combined}} = \sqrt{\sigma_{\mathrm{mean,MIPAS}}{}^2 + \sigma_{\mathrm{mean,comp}}{}^2} \quad (6)$$

were examined to estimate if the given errors are realistic (cf. von Clarmann, 2006). If the combined error is smaller than the standard deviation of the differences this hints at error estimates being too small, e.g. if not all sources of errors are considered or the retrieval error is underestimated. Since the measurements are not taken exactly at the same location and time, natural variability also contributes to differences between the combined error and the standard deviation.

For comparisons to the HATS network, MIPAS Envisat measurements at 3 km below the tropopause are used. The altitude where the tropopause is located was calculated from each MIPAS Envisat temperature profile as follows:

- Between 25° S and 25° N the altitude at 380 K potential temperature was used
- At higher latitudes the WMO criterion was used, e.g. the altitude where the vertical temperature gradient drops below 2 K km^{-1} and remains that small within a layer of 2 km

AMTD
8, 7573–7662, 2015

The value at 3 km below that altitude is chosen for each MIPAS profile. Cases for which the estimation of the tropopause height went obviously wrong were rejected. All available MIPAS Envisat measurements are used. To increase comparability of the data sets, monthly zonal means were calculated from MIPAS Envisat measurements in 10° bins. In addition, these zonal means (and their standard deviation) were weighted with the cosine of the latitude to simulate the approach performed for the HATS data.

Since some of the MIPAS Envisat detectors were shown to have time-dependent non-linearity correction functions due to detector aging (Eckert et al., 2014) we estimated drifts caused by this feature from a small subset of data. The comparison with HATS exhibits differences in the trends of MIPAS Envisat and the HATS time series. We compared the differences in these trends with the drift estimated due to detector aging. For the latter we calculated the mean drift by interpolating the drifts to 3 km below the tropopause and weighting them with the cosine of the latitude.

4 Validation results

In order to ensure good quality of the MIPAS Envisat CFC-11 and CFC-12 products, we compared the profiles with coinciding ones of several other instruments, e.g. Cryosampler, MkIV, MIPAS-B, MIPAS-STR, HIRDLS and ACE-FTS and also with measurements of the HATS network. The comparisons were performed by applying the validation schemes described in Sect. 3. The results of these comparisons are discussed in the following, first for CFC-11 and, subsequently, for CFC-12. The mean distance and time for the comparisons based on collocated measurements (e.g. with MIPAS-STR, HIRDLS, ACE-FTS and ILAS-II) are shown in Table 2.

AMTD
8, 7573–7662, 2015

4.1 CFC-11: reduced spectral resolution period (RR)

4.1.1 Results CFC-11: Cryosampler

Several MIPAS Envisat profiles are compared to those of Cryosampler (Fig. 1). For each Cryosampler profile (black dots), several MIPAS Envisat profiles meet the coincidence criteria (blue-greyish lines). The latter cover a considerable range of variability. The closest MIPAS Envisat profile (blue solid line) matches the Cryosampler profile remarkably well in all 5 cases, with maximum differences of 30 pptv (~ 13 %), except for the 10–15 km region on 3 October 2009 (right column, bottom panel). In addition, the mean of all coincident MIPAS Envisat profiles (red line) agrees reasonably well with the Cryosampler profile, suggesting that the air within the entire region meeting the coincidence criteria is decently represented by Cryosampler. Contrary to that, the respective seasonal zonal mean of MIPAS Envisat measurements (light orange line) occasionally deviates considerably from the actual measurements, particularly on 1 April 2011. This confirms that both, Cryosampler and MIPAS Envisat, can reliably detect atmospheric conditions deviating largely from the climatological state. In this particular case strong stratospheric subsidence has led to extraordinarily low mixing ratios of CFCs. This uncommon atmospheric situation went along with excessive ozone destruction (Manney et al., 2011; Sinnhuber et al., 2011).

4.1.2 Results CFC-11: MarkIV

Only one measurement of the balloon borne MkIV instrument (black line in Fig. 2) coincides with MIPAS Envisat measurements during the RR period. Three collocated profiles of MIPAS Envisat (blue-greyish lines) were found, of which also the mean profile (red line) and the closest profile (blue line) are shown. Up to approximately 25 km the MkIV profile reports higher mixing ratios than all of the MIPAS Envisat profiles, especially compared with the closest MIPAS Envisat profile. However, the gradient of the MkIV profile and all MIPAS Envisat profiles is very much alike between ~ 17 and

AMTD
8, 7573–7662, 2015

24 km. Contradictory to the comparison with Cryosampler, the closest MIPAS Envisat profile is furthest away from the MkIV profile throughout the whole altitude range. While the 3 collocated measurements lie within the MkIV error bars from the lower end of the profiles up to ∼ 17 km, this is generally not the case from that altitude upwards, but only around the crossing point of the MkIV profile with the MIPAS Envisat profiles at about 25–26 km. Up to that altitude the MkIV profile exhibits higher mixing ratios of CFC-11 than MIPAS Envisat, while above MkIV shows lower, mostly negative values. However, the differences with the MIPAS Envisat mean profile rarely exceed 20 pptv except for around 20 km where we find deviations of up to 30 pptv. This corresponds to less than 10 % at the lower end of the profile and up to 15 % around 20 km. Velazco et al. (2011) found similar differences in their comparisons of ACE-FTS and MkIV, which are based on noncoincident validation using a Potential Vorticity/Potential Temperature (PV/Theta) coordinate system (Manney et al., 2007). They also find largest deviations of the profiles around or slightly below 20 km, with maximum differences of up to ∼ 18 % and minimum differences in the order of ∼ 5 % around 17 km. Above 20 km, the mean profile of MIPAS Envisat and the MkIV profile agree well. Differences mainly stay within 10 %, except for above 26 km where MkIV mixing ratios become negative. Considering the small number of coincident MIPAS Envisat profiles (3), the instruments agree reasonably well below 20 km and good between 20 and 26 km.

4.1.3 Results CFC-11: MIPAS-B

For the comparison with two independent measurements of MIPAS-B, trajectory corrected profiles of the instrument were used (Fig. 3). In the comparison for the MIPAS-B flight of 24 January 2010 the agreement with MIPAS Envisat is remarkably good above ∼ 18 km, while below this altitude the mean profile of all collocated MIPAS Envisat measurements (Fig. 3: upper left panel; solid red line) shows higher values than the MIPAS-B profile (solid black line). However, the values of all collocated MIPAS Envisat profiles (red squares) cover a wider range, such that the MIPAS-B profile lies within their spread at all altitudes. The profiles deviate by approximately 30 pptv (∼ 30 %) at

AMTD
8, 7573–7662, 2015

the largest around 16–17 km (middle and right panel) and stay within 20 pptv (corresponding to ∼ 10 % at the lower end of the profile) for the rest of the covered altitude range. Throughout the whole vertical extent, MIPAS Envisat shows higher mixing ratios of CFC-11. However, the bias does not exceed the standard deviation of the differences. Large percentage errors above 19 km occur due to division by very small absolute amounts of CFC-11 at these altitudes. The MIPAS Envisat profile is smoother, supposedly due to several profiles being averaged to a mean profile.

The flight on 31 March 2011 (Fig. 3, lower panels) supports the conclusions drawn from the first comparison. Maximum differences are of similar magnitudes (around 30 pptv at the largest). However, the largest deviations between the MIPAS Envisat mean profile and the measurements of MIPAS-B appear at altitudes around 13 km, and exceed the standard deviation of the differences. Around 17 km a second peak occurs in the differences, which is at similar altitudes as for the first comparison. In general, both comparisons support the impression of MIPAS Envisat showing slightly higher values of CFC-11 below ∼ 18 km, even though the MIPAS-B profile is still enclosed within the spread of all MIPAS Envisat collocated profiles (left panel: red squares). The shape of the profiles, in terms of slope and reversal points, agrees well for both comparisons. Differences might be due to horizontal viewing direction and/or horizontal smoothing by the MIPAS-B measurement, since the observations are combined using trajectories which are associated with the localized coordinates. This is most important in the presence of pronounced atmospheric structures and strong gradients, e.g. the mixing barrier associated with the polar vortex.

4.1.4 Results CFC-11: MIPAS-STR

Seven profile pairs of collocated measurements were found for comparisons of MIPAS Envisat with MIPAS-STR (Fig. 4). The comparison is performed using mean profiles, rather than comparing each set of collocated pairs. Since MIPAS-STR profiles were originally sampled on a finer altitude grid (left panel; steel blue line) than MIPAS Envisat profiles (red line), these profiles were interpolated onto the MIPAS Envisat grid (black

AMTD
8, 7573–7662, 2015

line). The agreement of the profiles is good and the vertical structure is similar, showing minimum values around 16–17 km for both instruments. Differences are largest at the bottom end of the profiles at 8 km (middle panel). However, they do not exceed 30 pptv (corresponding to up to ∼ 15 % below 12 km and and up to ∼ 20 % around 14 km at the largest) throughout the rest of the profile and are not significant for the majority of the altitude levels. Above 14 km, the differences mainly stay within 10 pptv corresponding to ∼ 3–15 %. The mean difference oscillates around zero, which is most pronounced at altitudes below ∼ 15 km. The standard deviation of the differences (right panel; brown line) exceeds the estimated combined error (purple line). This reflects the fact that only the retrieval noise is shown and thus the error budget is incomplete. Atmospheric variability for the region fulfilling the coincidence criteria might also lead to differences which are not included in the combined error, even though the mean distance and time difference are only about 170 km and 1:45 h, respectively (comp. Table 2).

4.1.5 Results CFC-11: HIRDLS

The results of the comparison of MIPAS Envisat CFC-11 with that of HIRDLS are displayed in Figs. 5–7. Figure 5 shows that the HIRDLS profiles scatter the most at the ends of the profiles, e.g. at rather high altitudes (around ∼ 30 km; blue-greenish points) and the lower-most altitudes (around ∼ 10 km; red-yellowish points). It is also apparent that the measurements of HIRDLS CFC-11 cover a large range of values at all altitudes, which is evident in the large scatter throughout the whole vertical extent, with the largest spread at the lower end of the profiles, i.e. at high CFC-11 mixing ratios. Negative CFC-11 values do not exist in the HIRDLS results because the retrieval for the volume mixing ratio is logarithmic. The histograms shown in Fig. 6 give a more detailed picture of the frequency distributions of the CFC-11 mixing ratios of MIPAS Envisat (top panels) and HIRDLS (bottom panels) measurements at 16 km (left panels) and 23 km (right panels). In both cases MIPAS Envisat seems to see a bi-modal distribution (which is much more pronounced at 23 km), while HIRDLS only exhibits one obvious peak at 16 km and a slight bump, which seems to be a smeared out second mode, at

AMTD
8, 7573–7662, 2015

23 km. In both cases HIRDLS does not see the distinct second mode at higher values visible in MIPAS Envisat measurements around 250 pptv at 16 km and around 150 pptv at 23 km. The peak at lower mixing ratios appears around similar values for both instruments, slightly below 200 pptv at 16 km and between 0 and 50 pptv at 23 km. The maximum is shifted slightly towards lower mixing ratios in the case of HIRDLS. The comparison of the mean profiles (Fig. 7, left panel), which are calculated from more than 90 000 collocated profiles of HIRDLS (black) and MIPAS Envisat (red) over all latitudes, shows good agreement of the two instruments down to ∼ 16 km. Deviations stay within 10–15 pptv above this altitude. Below, MIPAS Envisat continuously shows higher mixing ratios of CFC-11 than HIRDLS (middle panel), with differences reaching as high as 60 pptv at the bottom end of the profile. This supposedly reflects the more pronounced second mode in the MIPAS Envisat frequency distribution (Fig. 6). However, MIPAS Envisat CFC-11 mixing ratios are no more than 40 pptv (∼ 20 %) larger than those of HIRDLS at altitude ranges between 9 and 16 km. In the left panel, the error bars shown for MIPAS Envisat include only the average retrieval noise, while HIRDLS error bars represent an estimated error, derived from 10 sets of 12 consecutive profiles at regions of little variability (Gille et al., 2014). The incomplete error budget leads to considerable differences between the combined error of the instruments (right panel, purple line) and the standard deviation of the differences. The covered vertical range of the combined error is smaller, since HIRDLS error estimates were only given for these altitude levels. It is also plausible that natural variability plays a role in the differences between the combined error and the standard deviation of the differences since both instruments did not measure exactly the same air mass. Due to the fact that the coincidence criteria allow for certain differences in time and geolocation the mean distance between the collocated measurements is approximately 200 km and the time difference is nearly 3 h (comp. Table 2). However, this effect is presumably minor compared to e.g. ACE-FTS for which the mean distance and time difference are about twice as large as for HIRDLS. At the bottom end of the profiles, the largest deviations of the mean profiles of MIPAS Envisat and HIRDLS can be found. Overall, the agreement of MIPAS Envisat

AMTD
8, 7573–7662, 2015

and HIRDLS CFC-11 measurements is excellent down to approximately 15 km. Below that altitude, MIPAS Envisat exhibits a slight high bias.

4.1.6 Results CFC-11: ACE-FTS

The correlation between MIPAS Envisat and ACE-FTS CFC-11 measurements (Fig. 8) is very close to linear, even though MIPAS Envisat seems to see slightly higher CFC-11 values in general. This is most obvious at higher CFC-11 mixing ratios, e.g. at lower altitudes (red-yellowish points) where the correlation is slightly off the 1 : 1 relation. The values do not scatter as much as for HIRDLS, presumably due to the fact that in the case of ACE-FTS the signal to noise ratio is better, since it measures in occultation and a large part of the HIRDLS aperture got blocked. The distribution of the mixing ratios at 16 km (Fig. 9: left panels) and 23 km (right panels) agree reasonably well for the two instruments. The skewness is very similar for both instruments, but the multimodal scheme is more pronounced for ACE-FTS at 16 km. A frequency maximum of mixing ratios appears slightly below 200 pptv in the case of MIPAS Envisat and between 150 and 200 pptv in the case of ACE-FTS. There is a second peak around 250 pptv in the ACE-FTS measurements which is less pronounced in the MIPAS Envisat values. At 23 km, both instruments show a bi-modal distribution of the mixing ratios, with values peaking between 0 and 50 pptv and close to 150 pptv. The ACE-FTS frequency distribution exhibits an additional peak at negative values, which are unphysical. 23 km is the upper limit of the ACE-FTS CFC-11 retrieval for the polar region. For these occultations, the spectrum supposedly contains little CFC-11 signal near 23 km and the retrieval is possibly compensating for some effect (e.g. bad residual from one of the interferers, mild channelling in the interferometer, a contribution to the spectral region from the aerosol layer) by giving negative CFC-11 mixing ratios. Similar as for HIRDLS, the main mode at 23 km is shifted to slightly lower values in the case of ACE-FTS compared to MIPAS Envisat. The figure of the mean profile comparison (Fig. 10) supports the conclusion from Fig. 8 that MIPAS Envisat sees higher volume mixing ratios of CFC-11. This is most pronounced at lower altitudes, approximately below ~ 17–18 km

AMTD
8, 7573–7662, 2015

(left and middle panel), where MIPAS Envisat CFC-11 mixing ratios (red line) are about 20 pptv (less than 10 %) higher than those of ACE-FTS, both compared to ACE-FTS on its original grid (steel blue line) and interpolated onto the MIPAS Envisat grid (black line). Again, MIPAS Envisat error bars represent the retrieval noise, while the ACE-FTS errors were estimated directly from the fit residual. The right-hand panel shows that the combined error (purple line) is far smaller than the standard deviation of the differences (brown line) for almost the complete altitude range. This suggests that for one of the instruments, or both, the error budget is considerably underestimated or incomplete (e.g. only retrieval noise in the case of MIPAS Envisat), or that natural variability was large. The latter plays a more important role than for e.g. HIRDLS, since the coincidence criteria for ACE-FTS with MIPAS Envisat are considerably less strict compared to those of HIRDLS and the mean distance and mean time difference are about 350 km and more than 6 h, respectively (comp. Table 2) and thus are about twice as large as those of HIRDLS.

Around 25 km (left panel) one can see a feature not known from any previous CFC-11 profiles, represented as a bump of suddenly increasing values. This increase in CFC-11 around 25 km does not originate from an actual atmospheric state, but is simply a sampling issue. ACE-FTS profiles are cut off at the upper end, when the mixing ratios become too small to be retrieved satisfactorily. Since CFC-11 values are largest in the tropics, the profiles are cut-off at higher altitudes than in polar regions, i.e. above 23 km only tropical – higher – values are shown. But Fig. 10 shows the global mean of all collocated ACE-FTS and MIPAS Envisat profiles. Hence, around 25 km the mean is suddenly more strongly dominated by tropical profiles, dragging it to higher values. Furthermore, it is admittedly not intuitive that regridding systematically adds a bias to the ACE-FTS profiles (interpolation from steel blue to black line). This shift towards mixing ratios valid at approximately 0.5 km below does not appear in the interpolated single profiles but only in the mean of the interpolated profiles. This is a pure sampling effect caused by the same mechanism as the artificial bump explained above: due to

AMTD
8, 7573–7662, 2015

the resampling on the MIPAS Envisat grid, the ACE-FTS cut-off altitude – and thus the bump – are shifted 500 m downwards.

Overall the MIPAS Envisat and ACE-FTS CFC-11 measurements agree reasonably well, not contradicting the conclusion from other comparisons that MIPAS Envisat has a slight high-bias at the lower end of the profile.

If the comparison is broken down into latitude bands (Fig. A2) the bump disappears. In addition, this breakdown into several latitude bands indicates that the tendency of MIPAS Envisat to detect higher amounts of CFC-11 at the lower end of the profile is more pronounced at higher latitudes. This feature is also visible in latitudinal breakdown of the comparison with HIRDLS (comp. Fig. A1).

Also interesting is the behavior of the tropical profiles in these figures. Compared to ACE-FTS, the MIPAS Envisat profile shows slightly increasing CFC-11 mixing ratios up to ∼ 15 km. An increase, from the bottom of the profile upwards, is also visible in ACE-FTS, but it is far less pronounced. The latitudinal breakdown for HIRDLS and MIPAS Envisat, shows that this increase is most pronounced in HIRDLS. This behavior of the mean profile is suspicious, since CFC-11 mixing ratios are expected to be constant throughout the troposphere, since it is well mixed, which might hint at problems concerning the retrieval and/or spectroscopical data in this region.

4.1.7 Results CFC-11: HATS

The high bias of MIPAS Envisat CFC-11 below approximately 15–17 km detected so far is further quantified by comparison to ground-based measurements of the HATS network (Fig. 11). Similar mixing ratios of stable source gases are to be expected at the surface and in the upper troposphere. Instead, the mean of the MIPAS Envisat measurements (continuous red line with large red circles) is about 10–15 pptv (∼ 5 %) higher than the mean of the data collected by the HATS network (continuous black line). Since the troposphere is well mixed, these values should agree well, which indicates a slight high-bias of the MIPAS Envisat measurements. Both, MIPAS Envisat and the HATS data, exhibit a descending slope in their time series, but the decrease

AMTD
8, 7573–7662, 2015

in MIPAS Envisat measurements seems to be slightly steeper. This effect is slightly more pronounced than the estimated drift at this altitude (comp. Fig. 16, left panel). Absolute drifts due to detector aging at 3 km below the tropopause were estimated to be $-3.58\,\mathrm{pptv\,decade^{-1}}$. This drift estimated from the difference in the trend in Fig. 11 is $-6.66\,\mathrm{pptv\,decade^{-1}}$ (comp. Sect. 3 for details on the method). So only part of the difference in the trends can be explained by the drift resulting from detector aging. However, the drift estimate due to detector aging is only based on drifts between 35° S and 35° N, due to lack of data, while the trends in the comparison with HATS result from measurements with almost pole to pole coverage. Thus, the comparison between the drift due to detector aging and the difference in the trends can only serve as an approximation. The amplitude of periodic variations is slightly more pronounced in MIPAS Envisat measurements, but qualitatively both instruments agree well. The standard deviation of the MIPAS Envisat data (dashed red line with small red circles) shows that the spread is rather large which is not surprising, considering that the mean includes global MIPAS Envisat measurements, which have a wider spread. Even though some HATS data lie within the standard deviation of the MIPAS Envisat measurements, the difference is obviously systematic.

4.2 CFC-11: high spectral resolution time period (FR)

Due to data availability we only compare MIPAS Envisat CFC measurements during the high spectral resolution period (FR) with those of MkIV, ACE-FTS, ILAS-LL and HATS.

4.2.1 Results CFC-11 V5H: MkIV

During the high spectral resolution (FR) period, two MkIV measurements are coincident with several MIPAS Envisat measurements (Fig. 12). While 16 MIPAS Envisat profiles were found to coincide with the MkIV profile taken on 16 December 2002, we find even 25 matches for the MkIV measurement taken on 1 April 2003. The color coding is

AMTD
8, 7573–7662, 2015

the same as in Fig. 2, showing collocated MIPAS Envisat measurements (blue-greyish lines), the mean of these profiles (red line) and the closest MIPAS Envisat profile (blue line) compared to the corresponding MkIV measurement (red line). The agreement is excellent up to 15–16 km with differences of less than 20 pptv (up to 10 %), while above that altitude MIPAS Envisat shows considerably higher values than MkIV for the 16 December 2002 measurement of MkIV. Above 21 km, MkIV even shows negative values at some altitude levels. The second comparison shows larger differences approximately around 15 km, but the agreement with the mean profile of the coincident MIPAS Envisat measurements is excellent below that altitude and up to about 20 km. Deviations of MkIV with the MIPAS Envisat mean profile range up to ∼ 30 pptv in both cases, while larger differences show up for comparisons to the closest MIPAS Envisat profile on 1 April 2003. These differences exceed 50 pptv around 15 km. However, the agreement between MIPAS Envisat and MkIV measurements of CFC-11 is similarly good for the FR and the RR period.

4.2.2 Results CFC-11 V5H: ACE-FTS

For the comparison of MIPAS Envisat CFC-11 with ACE-FTS 171 profile pairs matching the coincidence criteria were found during the FR period (Fig. 13). As in the case of the MIPAS Envisat RR data set, the ACE-FTS data were interpolated from their original grid (left panel: steel blue line) onto the MIPAS Envisat grid (black line) and were, after averaging, compared to MIPAS Envisat data (red line). Between 10 and 20 km the agreement between the two mean profiles is excellent, while below and above MIPAS Envisat shows higher mixing ratios of CFC-11. From 10 km upwards to 20 km, deviations of the mean profiles mostly stay within 10–20 pptv (middle panel), corresponding to ∼ 5 % around 10 km and ∼ 30 % at the around 20 km. Above and below, the differences are larger and sometimes exceed 30 pptv. Even though the standard error of the differences is considerably larger than for the RR period (due to far fewer pairs of collocated profiles), it does not include zero for most of the covered altitude range, indicating that the deviation of the profiles is still significant. As for the RR period, the

AMTD
8, 7573–7662, 2015

combined error of the instruments is underestimated, presumably mainly due to the fact that the error budget does not include all errors (e.g. only the retrieval noise in the case of MIPAS Envisat). Furthermore, the weak coincidence criterion allows for a, probably non-negligible, amount of natural variability to be included in the comparison.

Even though certain similarities with the MIPAS Envisat RR time period, like the known high-bias at the lower end of the profile, occur in the comparison of the MIPAS Envisat FR with ACE-FTS, the agreement between the two instruments is better than for the RR version in the region between 10 and 20 km which might be ascribed to the better spectral resolution of MIPAS Envisat during the FR period. However, the collocated measurements for the FR period consist only of profiles taken at higher northern latitudes. Thus the result may generally expose differences compared to the RR period, independently from differences due to the altered MIPAS Envisat retrieval setup, because the mean for the RR period consists of measurements over all latitudes and several years compared to only high latitude profiles taken during February and March 2004 for the FR period.

4.2.3 Results CFC-11 V5H: ILAS-II

About 5000 matches were found for the comparison of MIPAS Envisat CFC-11 measurements with ILAS-II (Fig. 14) during the FR period. However, apart from general turning points of the profile, the MIPAS Envisat (red line) and the ILAS-II mean profile (steel blue line: on its original grid; black line: on the MIPAS Envisat altitude grid) do not agree very well. Below 20 km, MIPAS Envisat shows higher mixing ratios of CFC-11 than ILAS-II and vice versa above that altitude. This feature has already been seen in other comparisons (comp. Wetzel et al., 2008), but the differences of MIPAS Envisat and ILAS-II exceed those of other comparisons by far. At the lower end of the profile, deviations go beyond 100 pptv (middle panel), which corresponds to relative differences of more than ~ 50 %, depending on the reference mixing ratio. Another conspicuous feature of this comparison are the very large error bars estimated from the ILAS-II retrieval (left panel: horizontal black and steel blue lines). However, Wetzel

AMTD
8, 7573–7662, 2015

et al. (2008) show similarly large error bars in their comparison of MIPAS-B with the former version of ILAS-II. Since the right panel of Fig. 14 demonstrates that the combined error of the two instruments (purple line) is far larger than the standard deviation of the differences (brown line), we suspect that the ILAS-II error is largely overestimated. Above 20 km, Wetzel et al. (2008) also found higher mixing ratios of CFC-11 in ILAS-II version 1.4 and version 2 measurements than in MIPAS-B, but no statement can be made about the lower end of the profile. Their compared ILAS-II profiles only reach down to ∼ 15/16 km (for version 1.4/version 2, respectively) and do not exhibit large deviations from MIPAS-B in this region, even though a slight indication of possible deviations at the lower end of the profile is visible from the 15 km grid point in ILAS-II version 1.4. All in all, the agreement of MIPAS Envisat CFC-11 measurements taken during the FR period with those of ILAS-II is not as good as for other instruments and shows far larger differences at the bottom end of the profile than comparisons with e.g. ACE-FTS or HATS. However, the results for the comparison with ILAS-II should be treated with care, since large differences with MIPAS-B and the former versions of ILAS-II have been found previously.

4.2.4 Results CFC-11 V5H: HATS

The comparison of MIPAS Envisat CFC-11 with HATS during the FR period covers less than two years (Fig. 15). This short time period, along with annual variations is an obstacle to the interpretation of the results. While the MIPAS Envisat time series (continuous red line with large red circles) oscillates around a relatively constant value during the measurement period, the HATS time series (black line) shows declining mixing ratios. Even though all values of the HATS measurements lie within the standard deviation of the MIPAS Envisat measurements a systematic deviation is still evident. The mixing ratios differ from values of about 10 pptv (∼ 4 %) at the beginning of the compared time series and to slightly larger values (around 5 %) at the end. While we consider the differences to be real, since the deviations are systematic and display

AMTD
8, 7573–7662, 2015

a similar picture as for the RR time period, we suggest to be careful not to overinterpret possible short term linear variations.

4.3 CFC-11 long-term stability

In order to verify the temporal stability of MIPAS Envisat CFC-11 measurements, drifts resulting from changing assumptions regarding the non-linearity correction (Fig. 16) were calculated. As shown by Eckert et al. (2014); Kiefer et al. (2013), the assumption of the non-linearity correction for the MIPAS Envisat detectors being time-independent cannot be held any more. Time-dependent coefficients for the non-linearity correction were found be able to explain drifts between MIPAS Envisat and other instruments, e.g. Aura MLS for ozone. Thus, the same method was used to calculate drifts in MIPAS Envisat CFC-11 measurements. MIPAS Envisat results produced using the retrieval setup for bulk processing are compared to results derived using newly suggested time-dependent non-linearity coefficients (comp. Eckert et al., 2014, Sect. 3.3). The difference between these results is calculated for a subset of measurements taken between June 2005 and October 2011. Subsequently, the temporal development of these differences is assessed by fitting a linear variation to them. The left panel in Fig. 16 shows an altitude–latitude cross-section of the estimated drifts, where bluish tiles indicate that MIPAS Envisat is seeing more negative/less positive trends using the old, not time-dependent, non-linearity coefficients. Red tiles indicate that MIPAS Envisat is seeing more positive/less negative trends for using the old setup. The drifts are very small compared to absolute mixing ratios of CFC-11, and only occasionally exceed 2 % decade^{-1}. Larger drifts appear exclusively at high latitudes in the Northern Hemisphere, which is a region with large natural variability and thus larger differences between the fit and the measurements lead to less reliable results. In order to prove that former results by Kellmann et al. (2012) are still valid, we compared the drift results with the trends for the whole MIPAS Envisat time series (Fig. 16, left panel). Reddish tiles indicate positive trends (only in the Southern Hemisphere between 25 and 30 km), while blueish tiles mean that the CFC-11 mixing ratios have decreased during the MIPAS Envisat

AMTD
8, 7573–7662, 2015

measurement period. Hatching indicates non-significant trends at 2-sigma level. While the trends are very small below ∼ 20 km (even ∼ 25 km in the tropics), negative trends of down to about −50 % were found above this altitude in the Northern Hemisphere. Positive trends range up to ∼ 20 %. These trends are by far larger than the estimated drifts and thus the conclusions drawn from these trends by Kellmann et al. (2012) still hold.

4.4 CFC-12

This section is dedicated to the results of the comparisons of MIPAS Envisat CFC-12 measurements with those of Cryosampler, MkIV, MIPAS-B, MIPAS-STR, HIRDLS, ACE-FTS and the HATS network (Figs. 17–27).

4.4.1 Results CFC-12: Cryosampler

For CFC-12, as well as for CFC-11, Cryosampler measurements (Fig. 17: black dots) were compared to MIPAS Envisat measurements. MIPAS Envisat measurements fulfilling the coincidence criteria (blue-greyish lines) exhibit a widely spread set of profiles enclosing the Cryosampler measurements. In most of the cases deviations of Cryosampler and the mean collocated MIPAS profile stay within 50 pptv (corresponding to ∼ 10 % at the lower end of the profile and increasing above due to smaller absolute values of CFC-12). The closest of these collocated MIPAS Envisat profiles (blue line) agrees very well with the Cryosampler measurements. Only the Cryosampler measurement taken on 3 October 2009 exhibits some outliers, deviating considerably from all coincident MIPAS Envisat profiles at about 20–25 km, while the rest of this profile still agrees very well with all collocated MIPAS Envisat measurements. It is possible that Cryosampler captured variations due to laminae of small vertical extent here, which cannot be detected by MIPAS Envisat. While the mean of the collocated MIPAS Envisat profiles (red line) comes very close to the Cryosampler measurements as well as the closest MIPAS Envisat profile, except for the outliers just mentioned, the seasonal

AMTD
8, 7573–7662, 2015

latitudinal means of MIPAS Envisat (light orange lines) can differ considerably from the Cryosampler and the closest MIPAS Envisat profile, which provides proof of large natural variability. This is most pronounced for the comparison on 1 April 2011, as already observed for CFC-11, and is supposedly as well due to subsidence in the remarkably cold and stable Arctic polar vortex being present during that winter. So for CFC-12 as well, we can conclude that both instruments capture deviations from the mean state of the atmosphere well. Even though there are a few Cryosampler outliers not matching the MIPAS Envisat data, the CFC-12 Cryosampler measurements agree very well with those of MIPAS Envisat in general.

4.4.2 Results CFC-12: MarkIV

Comparisons of MIPAS Envisat CFC-12 with MkIV measurements exhibit a similar behavior as for CFC-11 (Fig. 18) up to slightly below 30 km. MkIV (black line) shows higher mixing ratios of CFC-12 than both the mean MIPAS Envisat profile (red line) and, even more pronounced, the closest MIPAS Envisat profile (blue line). The gradient of the profiles between ∼ 20 and 27 km is similar for all profiles. Above approximately 27 km, however, the MIPAS Envisat profiles are oscillating strongly, which is most apparent in the closest profile. The MkIV profile exhibits small wiggles above that altitude as well, but not as pronounced as any of the MIPAS Envisat profiles. Unlike for CFC-11, the MkIV profile does not show negative values in the comparison for CFC-12. Differences of the profiles stay within ∼ 50 pptv throughout most of the altitude range between the lower end of the profile up to approximately 27 km, except for levels around 20 km where differences sometimes come close to 100 pptv. These values correspond to 10–15 % for most of the profile below 27 km and slightly over 20 % around 20 km. Velazco et al. (2011) also find higher values of MkIV compared to ACE-FTS throughout their whole altitude comparison range with an indication of the largest differences occurring around 20 km. However, they only find differences of up to 15 %. Above 35 km, deviations between the MkIV profiles and the MIPAS Envisat profiles are noticeably larger. Up to that altitude, however, the comparison of MIPAS Envisat with MkIV CFC-12 mea-

AMTD
8, 7573–7662, 2015

surements shows reasonably good agreement, considering only 3 coincident MIPAS Envisat profiles were found.

4.4.3 Results CFC-12: MIPAS-B

Several MIPAS Envisat profiles coinciding with backward and forward trajectories of two MIPAS-B measurements taken over Kiruna (Sweden) in January 2010 and March 2011 (Fig. 19, upper and lower panels, respectively), were taken into account for CFC-12 validation with MIPAS-B. For the January 2010 MIPAS-B profile (Fig. 19 upper panels: black line), the agreement with the mean MIPAS Envisat profile (red line) is very good. The MIPAS-B profile is embedded in the spread of MIPAS Envisat collocated profiles (red squares) throughout the whole vertical range. At altitudes above 17 km, the agreement between MIPAS-B and MIPAS Envisat is remarkably good, showing differences smaller than 25 pptv and closing in to zero above 21 km (middle panel). Below 18 km, MIPAS Envisat shows slightly larger values of CFC-12, with differences of up to ~ 40 pptv (corresponding to ~ 10 %), at the largest. Below ~ 17 km, these differences are similar to the standard deviation of the instruments (middle and right panel) and considerably smaller above.

Large percentage errors above ~ 22 km occur due to small absolute values of CFC-12 from this altitude upwards. In the comparison with the MIPAS-B measurement taken in March 2011, MIPAS Envisat shows considerably higher mixing ratios of CFC-12 below 15 km and around 18 km (Fig. 19, lower panels). From 15 km upwards, the MIPAS-B profile and the MIPAS Envisat mean profile show good agreement in gradient and turning points of the profiles and above 18 km they also agree very well quantitatively. Deviations between MIPAS Envisat and MIPAS-B range up to ~ 75 pptv around 12–13 and 18 km (middle panel) in absolute values, corresponding to relative differences of approximately 15 and 30 %, respectively (right panel). However, except for these regions, the two instruments show differences smaller than the standard deviation of the differences. While the shape of the two profiles is far more similar in the first comparison (MIPAS-B flight in January 2010), correction of the less than perfect coinci-

AMTD
8, 7573–7662, 2015

dence, by using trajectories to collect collocated MIPAS Envisat measurements, might not have worked that well. This particular atmospheric situation (winter and spring of 2011) was characterized by extraordinarily low temperatures and a very stable vortex. Due to possibly sharp horizontal gradients, MIPAS-B might have captured an air parcel having different characteristics than the mean of all collocated MIPAS Envisat profiles, even though trajectory corrected collocated profiles were used. Thus deviations due to natural variability might still occur. Due to the latter, we persist in considering the agreement between the instruments very good for CFC-12.

4.4.4 Results CFC-12: MIPAS-STR

The comparison of MIPAS-STR and MIPAS Envisat mean profiles consists of 7 pairs of collocated measurements (Fig. 20). The mean profiles of MIPAS-STR (steel blue line: on original grid; black: interpolated onto the MIPAS Envisat grid) and MIPAS Envisat (red line) agree very well. The minimum occurs around the same altitudes (approximately 17 km) and both profiles show a similar behavior of decreasing CFC-12 volume mixing ratios from the bottom of the profile up to the minimum, even though the MIPAS Envisat profile oscillates slightly at altitudes below ~ 15 km. The difference oscillates around zero and is very similar in shape with the difference profile of CFC-11 (comp. Fig. 4: middle panel). This is due to the fact, that the same observations were used as in the case of CFC-11. The overall vertical distribution of CFC-11 and CFC-12 indicated by the MIPAS-STR observations fits well with the distribution of these species derived from the MIPAS Envisat observations. This is plausible, since the distribution of the CFCs in the lower stratosphere is predominantly altered by dynamic processes and the considered observations of both instruments cover horizontally extended regions (i.e. several degrees in latitude). Differences are largest around 11 km and exhibit deviations of more than 40 pptv, corresponding to approximately 10 % (middle panel). Except for this altitude, the differences are mostly insignificant and stay within 30–40 pptv at the largest (corresponding to less than 10 % at the lower end of the profile and less than 5 % at the upper end). Again, only the retrieval noise is shown for both

AMTD
8, 7573–7662, 2015

instruments due to which the combined error of the instruments is considerably smaller than the standard deviation of the differences. As mentioned in Sect. 4.1.4 natural variability might also play a role, even though the mean distance and time difference are rather small as for CFC-11 (comp. Table 2). Overall, the agreement of MIPAS-STR and MIPAS Envisat is excellent.

4.4.5 Results CFC-12: HIRDLS

Comparisons of MIPAS Envisat and HIRDLS measurements of CFC-12 are summarized in Figs. 21–23. Figure 21 shows the correlation between MIPAS Envisat and HIRDLS measurements. HIRDLS measurements have several outliers in CFC-12, which tend to occur more frequently at smaller mixing ratios/higher altitudes. However, it is still visible that the measured mixing ratios of MIPAS Envisat and HIRDLS are correlated linearly in general. Obvious differences appear in Fig. 22, where the frequency of the measured amounts of CFC-12 at 16 (left panels) and 23 km (right panels) is shown. While the distributions look very similar at 16 km, clear differences are visible at 23 km. At 16 km both measurements frequencies show only one peak, which is centered approximately between 450 and 500 pptv in the case of HIRDLS and is slightly shifted to higher values in the case of MIPAS Envisat, where the peak is rather centered around 500 pptv and exhibits a steeper histogram at higher mixing ratios. At 23 km one can clearly make out 3 peaks in the MIPAS Envisat distribution, while for HIRDLS this feature, even though still visible, is smeared out quite severely and thus the right-most peak is hardly discernible in the HIRDLS distribution. This also leads to a flatter frequency distribution for HIRDLS. The middle maximum peaks at similar amounts of CFC-12 for both instruments though and lies between 200 and 250 pptv. The comparison of the mean profiles of MIPAS Envisat (Fig. 23: red line) and HIRDLS collocated measurements (black line) are very much alike. The shape of the mean profiles, as well as their maxima and turning points are very similar, even though the MIPAS Envisat profile branches off at slightly lower altitudes and exhibits a sharper turn around 16 km. Higher volume mixing ratios of CFC-12, which MIPAS Envisat shows be-

AMTD
8, 7573–7662, 2015

low 17 km, stay mostly within ∼ 20 pptv (∼ 4 %) difference, except from the lowest value (middle panel). Between 18 and 25 km MIPAS Envisat seems to see smaller amounts of CFC-12 than HIRDLS, with differences of up to nearly 40 pptv (corresponding to approx. 10 %). From 25 to 30 km MIPAS Envisat CFC-12 volume mixing ratios agree excellently with those of HIRDLS and differences are generally smaller than 20 pptv, corresponding to ∼ 2.5 % around 25 km and up to 15 % above 30 km. The combined error of the instruments is considerably smaller than the standard deviation of the differences, since only the retrieval noise is shown in the case of MIPAS Envisat, such that the error budget is incomplete. As for other comparisons natural variability might also contribute to the difference, even though this effect is supposedly minor. The latitudinal broken down comparisons (comp. Fig. A3) exhibits similar features as for CFC-11. At higher latitudes deviations of the profiles at the bottom end seem larger than in tropical or subtropical regions. Overall the agreement between MIPAS Envisat and HIRDLS CFC-12 is excellent.

4.4.6 Results CFC-12: ACE-FTS

The comparison of ACE-FTS and MIPAS Envisat CFC-12 profiles is shown in Figs. 24–26. Figure 24 exhibits a very close to linear correlation of the measurements. The agreement of the two instruments appears to be quite good, with very few outliers even though MIPAS Envisat seems to see slightly higher values at large values, e.g. at the lower end of the profile. This impression is supported in Fig. 25, which shows the frequency of MIPAS Envisat (top panels) and ACE-FTS (bottom panels) at 16 (left panels) and 23 km (right panels). It exhibits considerable numbers of MIPAS Envisat CFC-12 measurements reporting volume mixing ratios of 500–600 pptv at 16 km, while ACE-FTS does not report appreciable numbers of CFC-12 values above 550 pptv. This leads to a far steeper histogram at higher mixing ratios in the ACE-FTS frequency distribution at 16 km, while the histogram at lower mixing ratios is more similar to that of MIPAS Envisat, even though it is still a bit steeper. The only obvious peak at this altitude occurs at similar volume mixing ratios for both instruments (around 450 pptv in

AMTD
8, 7573–7662, 2015

the case of ACE-FTS and between 450 and 500 pptv in the case of MIPAS Envisat). At 23 km both instruments clearly show a tri-modal distribution, peaking close to zero, around ∼ 250 pptv and around ∼ 450 pptv. While the leftmost peak appears to be more pronounced in the ACE-FTS distribution, the middle and right peaks are very similar. The impression of MIPAS Envisat seeing higher values of CFC-12 at the lower end of the profile is confirmed in Fig. 26 as well. While the MIPAS Envisat (red line) and the ACE-FTS profiles (steel blue line: on original grid; black line: interpolated onto the MIPAS Envisat grid) are very close together at the bottom end (around ∼ 6 km), the MIPAS Envisat profile exhibits a steeper ascent than the ACE-FTS profiles, leading to deviating profiles of the instruments up to 18 km. Here, the MIPAS Envisat mean profile exhibits values of CFC-12 which are up to 25–30 pptv (6–7 %) higher than those of ACE-FTS (middle panel). From 18 up to ∼ 27–28 km MIPAS Envisat and ACE-FTS agree remarkably well with deviations of approximately 10 pptv, corresponding to ∼ 3 % around 18 km and less than 10 % around 27 km. Above these altitudes, ACE-FTS shows higher values of CFC-12 than MIPAS Envisat. Around 30 km the comparison exhibits the largest deviations appearing in differences of up to 50 pptv and more (which corresponds to ∼ 25 % and more at these altitudes). The comparison of the estimated precision and the standard deviation of the differences (right panel) shows that there is a large difference between these quantities almost throughout the whole altitude range. This is, to a large extent, due to the fact that only the retrieval noise is included for MIPAS Envisat. In addition, large natural variability cannot be ruled out as a cause. The latter might play a more important role than for the comparison with HIRDLS, since the HIRDLS coincidence criteria were chosen far stricter than for the comparison of MIPAS Envisat with ACE-FTS. The mean distance and time difference are similar to CFC-11 with about 375 km and 6 h, respectively (comp. Table 2). Both profiles show a bump, which is even more pronounced than for CFC-11. The explanation for this feature is the same as for CFC-11 and illustrates the sampling issue created by the combination of the cut-off of the ACE-FTS profiles at low CFC-12 values and the distribution of the gas, e.g. higher values at lower latitudes. Different to CFC-11, the bump is not

AMTD
8, 7573–7662, 2015

removed completely in the latitudinal breakdown (comp. Fig. A4). An indication of the bump at the upper end of the mean profiles is still visible at mid-latitudes, which is presumably attributed to high variability of CFC-12 within these bins. This originates from a similar sampling effect as for the whole set of measurements, just in smaller magnitude. At higher altitudes, the mean profile is again dominated by low latitude profile contributions, since profiles from higher latitudes are cut off at a lower altitude. As for the comparison with HIRDLS, we observe that differences at the lower end of the profile are largest at higher latitudes for CFC-12. Despite some differences, MIPAS Envisat and ACE-FTS CFC-12 measurements are in good agreement.

4.4.7 Results CFC-12: HATS

Similarly as for CFC-11, a comparison of HATS data with MIPAS Envisat measurements at an altitude of 3 km below the estimated tropopause was performed for CFC-12 as well (Fig. 27). This comparison suggests that MIPAS Envisat (continuous red line with large circles) detects slightly higher values than the HATS stations (continuous black line) at tropospheric levels. However, this effect seems to be less pronounced than for CFC-11. Deviations mainly stay within 10 pptv, which corresponds to $\sim 2\,\%$, since CFC-12 amounts are larger than for CFC-11. MIPAS Envisat's CFC-12 volume mixing ratios cover a wide range of values which is reflected in the large standard deviation (dashed red line with small circles) of approximately 30 pptv. The HATS time series are very close to the MIPAS Envisat measurements throughout the whole comparison period. Even though periodic variations in the MIPAS Envisat time series have larger amplitudes, the oscillations in both measurements agree with respect to their period and phase. Similar to CFC-11, there is an indication that the MIPAS Envisat CFC-12 time series is declining faster than that of HATS. The difference in the trends between MIPAS Envisat and HATS is $-6.85\,\mathrm{pptv\,decade^{-1}}$ (comp. Sect. 3 for details on the method). A similarly large drift ($-6.89\,\mathrm{pptv\,decade^{-1}}$) is found for results due to detector aging at 3 km below the tropopause. Hence, for CFC-12 the drift due to detector aging can explain the differences in the trends between MIPAS Envisat and HATS to

AMTD
8, 7573–7662, 2015

a large extend, even though only drifts between 35° S and 35° N contribute to the result due to detector aging because of lack of data. All in all, differences between the data sets are very small. Thus we consider the agreement to be very good.

4.5 CFC-12: High spectral resolution time period (FR)

4.5.1 Results CFC-12 V5H: MkIV

For the comparison of CFC-12 during the FR period, 15 collocated MIPAS Envisat profiles were found for the MkIV measurement taken on 16 December 2002 and 25 MIPAS Envisat profiles coincide with the MkIV measurement taken on 1 April 2003. The mean MIPAS Envisat profile (red line) and the MkIV profile (black line) are very close in both cases, showing deviations no larger than 50 pptv (corresponding to 10–20 % for most of the vertical range) and even a lot smaller at some altitude levels. Deviations with the closest MIPAS Envisat profile (blue line) are larger than for the mean profile, similar to the other comparisons with MkIV, ranging up to ∼ 100 pptv. There is a slight indication of the MkIV profile showing larger mixing ratios below 25 km in the second case, while this is not visible in the first one. However, the compared profiles show good agreement in general.

4.5.2 Results CFC-12 V5H: ACE-FTS

The comparison of MIPAS Envisat FR CFC-12 and ACE-FTS (Fig. 29) data is very similar to that of the reduced resolution period (RR: comp. Fig. 26), but the agreement is even better around ∼ 10–15 km. Since the comparison does not reach up beyond 28 km, the bump seen in the mean profiles for the RR period does not appear in either of the mean profiles for the FR period (left panel). This is mainly due to the fact that collocated measurements only exist at high latitudes for the short overlap of the ACE-FTS period and the MIPAS Envisat FR period. For most of the vertical range the differences stay within ∼ 10 pptv (middle panel), corresponding to ∼ 1 % at the lower

AMTD
8, 7573–7662, 2015

end of the profile and ∼ 20 % around 28 km. These values are only exceeded around ∼ 10 and 17–18 km, as well as at the lowest altitudes, where differences can reach up to 20–30 pptv (∼ 6 % below 13 km and less than 10 % around 17–18 km). While MIPAS Envisat shows slightly higher mixing ratios than ACE-FTS up to ∼ 14 km, it is vice versa above that altitude. Similar as for other comparisons of MIPAS Envisat and ACE-FTS throughout this paper, the combined error of the two instruments (right panel: purple line) is obviously smaller than the standard error of the differences (brown line). Explanations as mentioned before (comp. Sects. 4.1.6, 4.2.2 and 4.4.6) apply here as well. Overall, the agreement of MIPAS Envisat and ACE-FTS CFC-12 measurements is remarkably good for the MIPAS Envisat FR period.

4.5.3 Results CFC-12 V5H: ILAS-II

The comparison of MIPAS Envisat CFC-12 measurements from the FR period with ILAS-II measurements (Fig. 30) consists of about 5000 collocated profiles. Throughout the whole altitude range, with very few exceptions, ILAS-II (steel blue line: on its original grid; black line: on the MIPAS Envisat altitude grid) shows higher mixing ratios of CFC-12 than MIPAS Envisat (left panel: red line). But, while the mean profiles of MIPAS Envisat and ILAS-II agree rather well up to about 17 km, ILAS-II shows larger mixing ratios of CFC-12 above that altitude, which is most pronounced around 25 km. Apart from the lowermost two altitudes, the differences of the mean profiles do not exceed 50 pptv up to ∼ 17 km (middle panel), which corresponds to relative differences of approximately 10–15 % at the largest. From 17 km upwards however, deviations can be as large as close to 150 pptv around 25 km, resulting in relative differences of over 100 %, depending on which instrument is chosen as a reference. Wetzel et al. (2008) find a very similar behavior of ILAS-II version 2 measurements compared to MIPAS-B, with ILAS-II mixing ratios being larger over the whole altitude range and largest deviations of the two instruments above ∼ 20 km. As well as for CFC-11, the combined error of the two instruments exceed the standard deviations of the differences by far, which again leads to the conclusion that the large error bars shown in the left panel result

AMTD
8, 7573–7662, 2015

from an overestimated error budget for ILAS-II. Again, we suggest to treat conclusions drawn from the comparison with ILAS-II with care, since other instruments show very good agreement with MIPAS Envisat CFC-12 measurements during the FR period.

4.5.4 Results CFC-12 V5H: HATS

The short time series of the MIPAS Envisat FR period is compared to the measurements collected by the HATS network during the same time period for CFC-12 (Fig. 31). Similar as for CFC-11, MIPAS Envisat (continuous red line with large red circles) exhibits larger annual and interannual variations than the HATS data (continuous black line) from 2002 to the end of 2003. While MIPAS Envisat oscillates around a constant mixing ratio of approximately 550 pptv at 3 km below the tropopause, the HATS ground-based measurements show mixing ratios well within the range of 540–545 pptv. Thus, the difference between MIPAS Envisat and HATS are very small, at an order of ~ 10 pptv at the largest, which corresponds to relative differences of less than 2 %. According to this, we consider the agreement of MIPAS Envisat with HATS CFC-12 measurements to be remarkably good during the FR period.

4.6 CFC-12 long-term stability

The temporal stability over the whole MIPAS Envisat measurement period, was examined for CFC-12, as for CFC-11. The results of the drift estimation (Fig. 32) (left panel) exhibit small, even close to zero, negative drifts in CFC-12 below ~ 30 km. Above that altitude, up to ~ 35 km, larger negative drifts appear, which are largest at mid and high latitudes and range down to about −50 %. From 35 km upwards, large positive drifts were found which exceed 50 % at some points, with largest drifts shown at higher altitudes and latitudes. Compared to the trends (Fig. 32, right panel), the drifts are approximately of the same order of magnitude up to ~ 20 km (~ 25 km in the tropics). Between that altitude and ~ 30 km the trends are considerably larger and also show positive values in the Southern Hemisphere. From ~ 30–35 km negative trends are almost en-

AMTD
8, 7573–7662, 2015

tirely cancelled out by the drifts. This also applies to the positive trends above ~ 35 km. Keeping this in mind, the most pronounced trends are those between ~ 20 and 30 km, which have already been found and interpreted by Kellmann et al. (2012). Since drifts in this altitude range are very small, the conclusions drawn in their paper still hold. Above ~ 35 km, the apparent trend actually is a drift due to the time-dependent non-linearity of the detector which has not been accounted for in the bulk processing of the MIPAS Envisat data to date. After fixing this for the next data version, by using the new non-linearity correction coefficients, we assume the MIPAS Envisat CFC-12 data will be temporally stable throughout the whole vertical range.

5 Summary and conclusions

The MIPAS Envisat CFC-11 product shows good overall agreement with the presented collocated observations. A slight high-bias is found at low altitudes, below ~ 10 km for the FR period and ~ 15 km for the RR period. Except for a few outliers in the comparison with the Cryosamler measurement taken on 3 October 2009, the CFC-12 product exhibits excellent agreement with all compared instruments, for the RR data. Larger differences appear in the comparison with ILAS-II, but we suggest to treat these results with care since Wetzel et al. (2008) found similarly large differences when comparing MIPAS-B results to a former version of ILAS-II measurements. Differences in CFC-11 tend to be smaller than 50 pptv in most cases, which corresponds to approximately 20 % at the largest. In the case of CFC-12, maximum differences are similarly large in the absolute value of about 50 pptv, but since CFC-12 appears in larger amounts in the atmosphere than CFC-11 the relative deviations of MIPAS Envisat from comparison instruments are far smaller and hardly larger than 10 %. This value of relative differences is not even reached in most of the comparisons. After all, it becomes apparent that MkIV measurements are the only ones showing higher volume mixing ratio than MIPAS Envisat at the lower end of the profiles. The combined retrieval noise is almost always smaller than the standard deviation of the differences, indicating that the error

AMTD
8, 7573–7662, 2015

budget is incomplete and that unaccounted random-type errors or natural variability contribute to the detected differences.

Estimated drifts are small for both species below ∼ 25–30 km. Above that altitude CFC-11 is difficult to detect and the test data set for drift estimates from different non-linearity correction coefficients was sparse, so that no results exist from ∼ 25 km upwards. CFC-12 drifts reach up to magnitudes of about 50 % above ∼ 30 km, showing large negative values up to ∼ 35 km and positive values above. This is reflected in the trend, which is mostly artificial above this altitude. At 3 km below the tropopause the drift can partly explain the differences in the trends between MIPAS Envisat and ground-based HATS CFC-11 data. For CFC-12 the drift is very similar to the differences found in the trends of MIPAS Envisat at 3 km below the tropopause and the HATS measurements and is thus a good candidate for explaining these differences. For future data versions these results will be taken into account to produce a temporally stable CFC-12 data set, which will then be also suitable to trend analysis above 35 km.

Appendix

In order to have a closer look at the latitudinal dependence of the differences, we broke the comparison vs. HIRDLS and ACE-FTS down into 5 latitude bands. We did not do this for the comparisons with other instruments because most of them lack global coverage.

Acknowledgements. The retrievals of IMK/IAA were partly performed on the HP XC4000 of the Scientific Supercomputing Center (SSC) Karlsruhe under project grant MIPAS. IMK data analysis was supported by DLR under contract number 50EE0901. MIPAS level 1B data were provided by ESA. We acknowledge support by Deutsche Forschungsgemeinschaft and Open Access Publishing Fund of Karlsruhe Institute of Technology. The Atmospheric Chemistry Experiment (ACE), also known as SCISAT, is a Canadian-led mission mainly supported by the Canadian Space Agency and the Natural Sciences and Engineering Research Council of Canada.

AMTD
8, 7573–7662, 2015

Work at the Jet Propulsion Laboratory, California Institute of Technology, was carried out under contract with the National Aeronautics and Space Administration. Data collection and analysis of MIPAS-STR data used here were supported by the EU-project RECONCILE (grant No. 15 226365-FP7-ENV-2008-1) and the BMBF-project ENVIVAL-Life (DLR grant no. 50EE0841). Balloon flights and data analysis of MIPAS-B data used here were supported by the European Space Agency (ESA), the German Aerospace Center (DLR), CNRS (Centre National de la RechercheScientifique), and CNES (Centre National d'Etudes Spatiales). The ILAS-II project was funded by Ministry of the Environment of Japan.

References

Bernath, P. F., McElroy, C. T., Abrams, M. C., Boone, C. D., Butler, M., Camy-Peyret, C., Carleer, M., Clerbaux, C., Coheur, P.-F., Colin, R., DeCola, P., De Mazière, M., Drummond, J. R., Dufour, D., Evans, W. F. J., Fast, H., Fussen, D., Gilbert, K., Jennings, D. E., Llewellyn, E. J., Lowe, R. P., Mahieu, E., McConnell, J. C., McHugh, M., McLeod, S. D., Michaud, R., Midwinter, C., Nassar, R., Nichitiu, F., Nowlan, C., Rinsland, C. P., Rochon, Y. J., Rowlands, N., Semeniuk, K., Simon, P., Skelton, R., Sloan, J. J., Soucy, M.-A., Strong, K., Tremblay, P., Turnbull, D., Walker, K. A., Walkty, I., Wardle, D. A., Wehrle, V., Zander, R., and Zou, J.: Atmospheric Chemistry Experiment (ACE): mission overview, Geophys. Res. Lett., 32, L15S01, doi:10.1029/2005GL022386, 2005. 7585

Boone, C. D., Nassar, R., Walker, K. A., Rochon, Y., McLeod, S. D., Rinsland, C. P., and Bernath, P. F.: Retrievals for the atmospheric chemistry experiment Fourier-transform spectrometer, Appl. Optics, 44, 7218–7231, 2005. 7586

Boone, C. D., Walker, K. A., and Bernath, P. F.: Version 3 retrievals for the Atmospheric Chemistry Experiment Fourier Transform Spectrometer (ACE-FTS), in: The Atmospheric Chemistry Experiment ACE at 10: A Solar Occultation Anthology, edited by: Bernath, P. F., A. Deepak Publishing, Hampton, Virginia, USA, 103–127, 2013. 7586

Brasseur, G. and Solomon, S.: Aeronomy of the Middle Atmosphere–Chemistry and Physics of the Stratosphere and Mesosphere, Atmospheric and Oceanographic Sciences Library 32, 3rd edn., Springer, Dordrecht, the Netherlands, 2005. 7576

Eckert, E., von Clarmann, T., Kiefer, M., Stiller, G. P., Lossow, S., Glatthor, N., Degenstein, D. A., Froidevaux, L., Godin-Beekmann, S., Leblanc, T., McDermid, S., Pastel, M., Steinbrecht, W.,

AMTD
8, 7573–7662, 2015

Swart, D. P. J., Walker, K. A., and Bernath, P. F.: Drift-corrected trends and periodic variations in MIPAS IMK/IAA ozone measurements, Atmos. Chem. Phys., 14, 2571–2589, doi:10.5194/acp-14-2571-2014, 2014. 7591, 7604, 7642

Elkins, J. W., Thompson, T. M., Swanson, T. H., Butler, J. H., Hall, B. D., Cummings, S. O., Fisher, D. A., and Raffo, A. G.: Decrease in the growth rates of atmospheric chlorofluorocarbons 11 and 12, Nature, 364, 780–783, 1993. 7588

Farman, J. C., Gardiner, B. G., and Shanklin, J. D.: Large losses of total ozone in Antarctica reveal seasonal ClO_x/NO_x interaction, Nature, 315, 207–210, 1985. 7577

Fischer, H. and Oelhaf, H.: Remote sensing of vertical profiles of atmospheric trace constituents with MIPAS limb-emission spectrometers, Appl. Optics, 35, 2787–2796, 1996. 7582

Fischer, H., Birk, M., Blom, C., Carli, B., Carlotti, M., von Clarmann, T., Delbouille, L., Dudhia, A., Ehhalt, D., Endemann, M., Flaud, J. M., Gessner, R., Kleinert, A., Koopman, R., Langen, J., López-Puertas, M., Mosner, P., Nett, H., Oelhaf, H., Perron, G., Remedios, J., Ridolfi, M., Stiller, G., and Zander, R.: MIPAS: an instrument for atmospheric and climate research, Atmos. Chem. Phys., 8, 2151–2188, doi:10.5194/acp-8-2151-2008, 2008. 7579

Friedl-Vallon, F., Maucher, G., Kleinert, A., Lengel, A., Keim, C., Oelhaf, H., Fischer, H., Seefeldner, M., and Trieschmann, O.: Design and characterisation of the ballon–borne Michelson Interferometer for Passive Atmospheric Sounding (MIPAS–B2), Appl. Optics, 43, 3335–3355, 2004. 7582

Gille, J., Barnett, J., Arter, P., Barker, M., Bernath, P., Boone, C., Cavanaugh, C., Chow, J., Coffey, M., Craft, J., Craig, C., Dials, M., Dean, V., Eden, T., Edwards, D. P., Francis, G., Halvorson, C., Harvey, L., Hepplewhite, C., Khosravi, R., Kinnison, D., Krinsky, C., Lambert, A., Lee, H., Lyjak, L., Loh, J., Mankin, W., Massie, S., McInerney, J., Moorhouse, J., Nardi, B., Packman, D., Randall, C., Reburn, J., Rudolf, W., Schwartz, M., Serafin, J., Stone, K., Torpy, B., Walker, K., Waterfall, A., Watkins, R., Whitney, J., Woodard, D., and Young, G.: High resolution dynamics limb sounder: experiment overview, recovery, and validation of initial temperature data, J. Geophys. Res.-Atmos., 113, D16S43, doi:10.1029/2007JD008824, 2008. 7584

Gille, J., Gray, L., Cavanaugh, C., Coffey, M., Dean, V., Halvorson, C., Karol, S., Khosravi, R., Kinnison, D., Massie, S., Nardi, B., Rivas, M. B., Smith, L., Torpy, B., Waterfall, A., and Wright, C.:, available at: http://www.eos.ucar.edu/hirdls/data/products/HIRDLS-DQD_V7-1.pdf, last access: 10 September 2014. 7584, 7585, 7596, 7633

AMTD
8, 7573–7662, 2015

Höpfner, M., Blom, C. E., Echle, G., Glatthor, N., Hase, F., and Stiller, G. P.: Retrieval simulations for MIPAS–STR measurements, in: IRS 2000: Current Problems in Atmospheric Radiation, edited by: Smith, W. L. and Timofeyev, Y. M., A. Deepak Publishing, Hampton, Va, USA, 1121–1124, 2001. 7583

Keim, C., Liu, G. Y., Blom, C. E., Fischer, H., Gulde, T., Höpfner, M., Piesch, C., Ravegnani, F., Roiger, A., Schlager, H., and Sitnikov, N.: Vertical profile of peroxyacetyl nitrate (PAN) from MIPAS-STR measurements over Brazil in February 2005 and its contribution to tropical UT NO_y partitioning, Atmos. Chem. Phys., 8, 4891–4902, doi:10.5194/acp-8-4891-2008, 2008. 7583

Kellmann, S., von Clarmann, T., Stiller, G. P., Eckert, E., Glatthor, N., Höpfner, M., Kiefer, M., Orphal, J., Funke, B., Grabowski, U., Linden, A., Dutton, G. S., and Elkins, J. W.: Global CFC-11 (CCl_3F) and CFC-12 (CCl_2F_2) measurements with the Michelson Interferometer for Passive Atmospheric Sounding (MIPAS): retrieval, climatologies and trends, Atmos. Chem. Phys., 12, 11857–11875, doi:10.5194/acp-12-11857-2012, 2012. 7577, 7578, 7579, 7604, 7605, 7616

Kiefer, M., Aubertin, G., Birk, M., De Laurentis, M., Eckert, E., Kleinert, A., Perron, G., and Wagner, G.: Impact of improved corrections for MIPAS detector non-linearity, in: Atmospheric Composition Validation and Evolution, Abstract Book, ESA, Frascati, 13–15 March 2013, p. 38, 2013. 7604

Laube, J. C., Engel, A., Bönisch, H., Möbius, T., Worton, D. R., Sturges, W. T., Grunow, K., and Schmidt, U.: Contribution of very short-lived organic substances to stratospheric chlorine and bromine in the tropics – a case study, Atmos. Chem. Phys., 8, 7325–7334, doi:10.5194/acp-8-7325-2008, 2008. 7581

Manney, G. L., Daffer, W. H., Zawodny, J. M., Bernath, P. F., Hoppel, K. W., Walker, K. A., Knosp, B. W., Boone, C., Remsberg, E. E., Santee, M. L., Harvey, V. L., Pawson, S., Jackson, D. R., Deaver, L., McElroy, C. T., McLinden, C. A., Drummond, J. R., Pumphrey, H. C., Lambert, A., Schwartz, M. J., Froidevaux, L., McLeod, S., Takacs, L. L., Suarez, M. J., Trepte, C. R., Cuddy, D. C., Livesey, N. J., Harwood, R. S., and Waters, J. W.: Solar occultation satellite data and derived meteorological products: sampling issues and comparisons with Aura Microwave Limb Sounder, J. Geophys. Res.-Atmos., 112, D24S50, doi:10.1029/2007JD008709, 2007. 7593

Manney, G. L., Santee, M. L., Rex, M., Livesey, N. J., Pitts, M. C., Veefkind, P., Nash, E. R., Wohltmann, I., Lehmann, R., Froidevaux, L., Poole, L. R., Schoeberl, M. R., Haffner, D. P.,

AMTD
8, 7573–7662, 2015

Davies, J., Dorokhov, V., Johnson, H. G. B., Kivi, R., Kyrö, E., Larsen, N., Levelt, P. F., Makshtas, A., McElroy, C. T., Nakajima, H., Parrondo, M. C., Tarasick, D. W., von der Gathen, P., Walker, K. A., and Zinoviev, N. S.: Unprecedented Arctic ozone loss in 2011, Nature, 478, 469–475, doi:10.1038/nature10556, 2011. 7592

McElroy, M. B., Salawitch, R. J., Wofsy, S. C., and Logan, J. A.: Reductions of Antarctic ozone due to synergistic interactions of chlorine and bromine, Nature, 321, 759–762, doi:10.1038/321759a0, 1986. 7577

Molina, L. T. and Molina, M. J.: Production of Cl_2O_2 from the self-reaction of the ClO radical, J. Phys. Chem. A, 91, 433–436, 1987. 7577

Molina, M. J. and Rowland, F. S.: Stratospheric sink for chlorofluoromethanes: chlorine atom–catalysed destruction of ozone, Nature, 249, 810–812, 1974. 7576

Montzka, S. A., Butler, J. H., Myers, R. C., Thompson, T. M., Swanson, T. H., Clarke, A. D., Lock, L. T., and Elkins, J. W.: Decline in the tropospheric abundance of halogen from halocarbons: implications for stratospheric ozone depletion, Science, 272, 1318–1322, doi:10.1126/science.272.5266.1318, 1996. 7588

Nakajima, H., Sugita, T., Yokota, T., Kobayashi, H., Sasano, Y., Ishigaki, T., Mogi, Y., Araki, N., Waragai, K., Kimura, N., Iwazawa, T., Kuze, A., Tanii, J., Kawasaki, H., Horikawa, M., Togami, T., and Uemura, N.: Characteristics and performance of the improved limb atmospheric spectrometer-II (ILAS-II) on board the ADEOS-II satellite, J. Geophys. Res., 111, D11S01, doi:10.1029/2005JD006334, 2006. 7587, 7588

Norton, R. H., and Beer, R.: New apodizing functions for Fourier spectrometry, J. Opt. Soc. Am., 66, 259–264, 1976. 7583

Oshchepkov, S., Sasano, Y., Yokota, T., Nakajima, H., Uemura, N., Saitoh, N., Sugita, T., and Matsuda, H.: ILAS data processing for stratospheric gas and aerosol retrievals with aerosol physical modeling: methodology and validation of gas retrievals, J. Geophys. Res., 111, D02307, doi:10.1029/2005JD006543, 2006. 7587

Piesch, C., Gulde, T., Sartorius, C., Friedl-Vallon, F., Seefeldner, M., Wölfel, M., Blom, C. E., and Fischer, H.: Design of a MIPAS instrument for high–altitude aircraft, in: Proc. 2nd International Airborne Remote Sensing Conference and Exhibition, ERIM, Ann Arbor, MI, 24–27 June 1996, vol. II, 199–208, 1996. 7582

Rodgers, C. D.: Inverse Methods for Atmospheric Sounding: Theory and Practice, vol. 2 of Series on Atmospheric, Oceanic and Planetary Physics, edited by: Taylor, F. W., World Scientific, 2000. 7584

AMTD
8, 7573–7662, 2015

Rothman, L. S., Jacquemart, D., Barbe, A., Benner, D. C., Birk, M., Brown, L. R., Carleer, M. R., Chackerian Jr., C., Chance, K., Coudert, L. H., Dana, V., Devi, V. M., Flaud, J.-M., Gamache, R. R., Goldman, A., Hartmann, J.-M., Jucks, K. W., Maki, A. G., Mandin, J.-Y., Massie, S. T., Orphal, J., Perrin, A., Rinsland, C. P., Smith, M. A. H., Tennyson, J., Tolchenov, R. N., Toth, R. A., Vander Auwera, J., Varanasi, P., and Wagner, G.: The HITRAN 2004 molecular spectroscopic database, J. Quant. Spectrosc. Ra., 96, 139–204, doi:10.1016/j.jqsrt.2004.10.008, 2005. 7587

Schmidt, U., Kulessa, G., Klein, E., Roeth, E.-P., and Fabian, P.: Intercomparison of balloon-borne cryogenic whole air samplers during the MAP/GLOBUS 1983 campaign, Planet. Space Sci., 35, 647–656, doi:10.1016/0032-0633(87)90131-0, 1987. 7580

Schoeberl, M. R., Douglass, A. R., Polansky, B., Boone, C., Walker, K. A., and Bernath, P.: Estimation of stratospheric age spectrum from chemical tracers, J. Geophys. Res., 110, D21303, doi:10.1029/2005JD006125, 2005. 7577

Sinnhuber, B.-M., Stiller, G., Ruhnke, R., von Clarmann, T., Kellmann, S., and Aschmann, J.: Arctic winter 2010/2011 at the brink of an ozone hole, Geophys. Res. Lett., 38, L24814, doi:10.1029/2011GL049784, 2011. 7592

SPARC Report No. 6: SPARC Report on the Lifetimes of Stratospheric Ozone-Depleting Substances, Their Replacements, and Related Species, edited by: Ko, M., Newman, P., Reimann, S., and Strahan, S., SPARC Report No. 6, WCRP-15/2013 2013. 7577

Stiller, G. P. (Eds.): The Karlsruhe Optimized and Precise Radiative Transfer Algorithm (KOPRA), vol. FZKA 6487 of Wissenschaftliche Berichte, Forschungszentrum Karlsruhe, Karlsruhe, Germany, 2000. 7579, 7583

Toon, G. C.: The JPL MkIV interferometer, Opt. Photonics News, 2, 19–21, 1991. 7581

Velazco, V. A., Toon, G. C., Blavier, J.-F. L., Kleinböhl, A., Manney, G. L., Daffer, W. H., Bernath, P. F., Walker, K. A., and Boone, C.: Validation of the atmospheric chemistry experiment by noncoincident MkIV balloon profiles, J. Geophys. Res., 116, D06306, doi:10.1029/2010JD014928, 2011. 7581, 7593, 7606

von Clarmann, T.: Validation of remotely sensed profiles of atmospheric state variables: strategies and terminology, Atmos. Chem. Phys., 6, 4311–4320, doi:10.5194/acp-6-4311-2006, 2006. 7590

von Clarmann, T., Oelhaf, H., and Fischer, H.: Retrieval of atmospheric O_3, HNO_3, CFC–11, and CFC–12 profiles from MIPAS–B–89 limb emission spectra, Appl. Optics, 32, 6808–6817, 1993. 7582

AMTD
8, 7573–7662, 2015

von Clarmann, T., Glatthor, N., Grabowski, U., Höpfner, M., Kellmann, S., Kiefer, M., Linden, A., Mengistu Tsidu, G., Milz, M., Steck, T., Stiller, G. P., Wang, D. Y., Fischer, H., Funke, B., Gil-López, S., and López-Puertas, M.: Retrieval of temperature and tangent altitude pointing from limb emission spectra recorded from space by the Michelson Interferometer for Passive Atmospheric Sounding (MIPAS), J. Geophys. Res., 108, 4736, doi:10.1029/2003JD003602, 2003. 7579

von Clarmann, T., Höpfner, M., Kellmann, S., Linden, A., Chauhan, S., Funke, B., Grabowski, U., Glatthor, N., Kiefer, M., Schieferdecker, T., Stiller, G. P., and Versick, S.: Retrieval of temperature, H_2O, O_3, HNO_3, CH_4, N_2O, $ClONO_2$ and ClO from MIPAS reduced resolution nominal mode limb emission measurements, Atmos. Meas. Tech., 2, 159–175, doi:10.5194/amt-2-159-2009, 2009. 7579

von Hobe, M., Bekki, S., Borrmann, S., Cairo, F., D'Amato, F., Di Donfrancesco, G., Dörnbrack, A., Ebersoldt, A., Ebert, M., Emde, C., Engel, I., Ern, M., Frey, W., Genco, S., Griessbach, S., Grooß, J.-U., Gulde, T., Günther, G., Hösen, E., Hoffmann, L., Homonnai, V., Hoyle, C. R., Isaksen, I. S. A., Jackson, D. R., Jánosi, I. M., Jones, R. L., Kandler, K., Kalicinsky, C., Keil, A., Khaykin, S. M., Khosrawi, F., Kivi, R., Kuttippurath, J., Laube, J. C., Lefèvre, F., Lehmann, R., Ludmann, S., Luo, B. P., Marchand, M., Meyer, J., Mitev, V., Molleker, S., Müller, R., Oelhaf, H., Olschewski, F., Orsolini, Y., Peter, T., Pfeilsticker, K., Piesch, C., Pitts, M. C., Poole, L. R., Pope, F. D., Ravegnani, F., Rex, M., Riese, M., Röckmann, T., Rognerud, B., Roiger, A., Rolf, C., Santee, M. L., Scheibe, M., Schiller, C., Schlager, H., Siciliani de Cumis, M., Sitnikov, N., Søvde, O. A., Spang, R., Spelten, N., Stordal, F., Sumińska-Ebersoldt, O., Ulanovski, A., Ungermann, J., Viciani, S., Volk, C. M., vom Scheidt, M., von der Gathen, P., Walker, K., Wegner, T., Weigel, R., Weinbruch, S., Wetzel, G., Wienhold, F. G., Wohltmann, I., Woiwode, W., Young, I. A. K., Yushkov, V., Zobrist, B., and Stroh, F.: Reconciliation of essential process parameters for an enhanced predictability of Arctic stratospheric ozone loss and its climate interactions (RECONCILE): activities and results, Atmos. Chem. Phys., 13, 9233–9268, doi:10.5194/acp-13-9233-2013, 2013. 7583

Wetzel, G., Sugita, T., Nakajima, H., Tanaka, T., Yokota, T., Friedl-Vallon, F., Kleinert, A., Maucher, G., and Oelhaf, H.: Technical Note: Intercomparison of ILAS-II version 2 and 1.4 trace species with MIPAS-B measurements, Atmos. Chem. Phys., 8, 1119–1126, doi:10.5194/acp-8-1119-2008, 2008. 7602, 7603, 7614, 7616

Wetzel, G., Oelhaf, H., Friedl-Vallon, F., Kleinert, A., Maucher, G., Nordmeyer, H., and Orphal, J.: Long-term intercomparison of MIPAS additional species $ClONO_2$, N_2O_5, CFC-

AMTD
8, 7573–7662, 2015

11, and CFC-12 with MIPAS-B measurements, Ann. Geophys.-Italy, 56, Fast Track-1, doi:10.4401/ag-6329, 2013. 7582

Woiwode, W., Oelhaf, H., Gulde, T., Piesch, C., Maucher, G., Ebersoldt, A., Keim, C., Höpfner, M., Khaykin, S., Ravegnani, F., Ulanovsky, A. E., Volk, C. M., Hösen, E., Dörnbrack, A., Ungermann, J., Kalicinsky, C., and Orphal, J.: MIPAS-STR measurements in the Arctic UTLS in winter/spring 2010: instrument characterization, retrieval and validation, Atmos. Meas. Tech., 5, 1205–1228, doi:10.5194/amt-5-1205-2012, 2012. 7583

Woiwode, W., Sumińska-Ebersoldt, O., Oelhaf, H., Höpfner, M., Belyaev, G. V., Ebersoldt, A., Friedl-Vallon, F., Grooß, J.-U., Gulde, T., Kaufmann, M., Kleinert, A., Krämer, M., Kretschmer, E., Kulessa, T., Maucher, G., Neubert, T., Piesch, C., Preusse, P., Riese, M., Rongen, H., Sartorius, C., Schardt, G., Schönfeld, A., Schuettemeyer, D., Sha, M. K., Stroh, F., Ungermann, J., Volk, C. M., and Orphal, J.: Validation of first chemistry mode retrieval results from the new limb-imaging FTS GLORIA with correlative MIPAS-STR observations, Atmos. Meas. Tech., 8, 2509–2520, doi:10.5194/amt-8-2509-2015, 2015. 7583

World Meteorological Organization: Scientific Assessment of Ozone Depletion: 2010, Global Ozone Research and Monitoring Project – Report No. 52, 516 pp., Geneva, Switzerland, 2011. 7577

World Meteorological Organization (WMO): Scientific Assessment of Ozone Depletion: 2014, Global Ozone Research and Monitoring Project – Report, World Meteorological Organization, No. 55, 416 pp., Geneva, Switzerland, 2014. 7578

Yokota, T., Nakajiama, H., Sugita, T., Tsubaki, H., Itou, Y., Kaji, M., Suzuki, M., Kanzawa, H., Park, J. H., and Sasano, Y.: Improved Limb Atmospheric Spectrometer (ILAS) data retrieval algorithm for Version 5.20 gas profile products, J. Geophys. Res., 107, 8216, doi:10.1029/2001JD000628, 2002. 7587

AMTD
8, 7573–7662, 2015

Table 1. Overview of the instruments and their important characteristics used for the validation of the MIPAS Envisat CFC-11 and CFC-12 products. ILAS-II is only used for the validation of the high spectral resolution (FR) period. ACE-FTS and MkIV are used to validate the MIPAS Envisat data from both periods, while the rest of the instruments only cover the reduced spectral resolution period.

		Envisat/ MIPAS (FR) RR	SCISAT/ ACE-FTS	Aura/ HIRDLS	ADEOS-II/ ILAS-II	MkIV	Cryosampler	MIPAS-B	HATS	MIPAS-STR
Platform		satellite	satellite	satellite	satellite	balloon	balloon	balloon	ground	airplane
Measurement type		limb emission	solar occultation	limb emission	solar occultation	solar occultation	in-situ sampling	limb emission	in-situ sampling	limb emission
Observation period		(2002–2004) 2005–2012 ~daily	since 2004 ~daily	2005–2008 ~daily	Dec 2002–Oct 2003	since 1989 ~ 22 flights	since 1982 ~ 50 flights	since 1989 24 flights	since 1977 monthly to hourly	since 1999 ~ 50 flights
CFC-11	coverage	~5–30 km	~6–27 km	~8–28 km	10–30 km	~5–38 km	~10–35 km	~10–30 km	surface	~5–20 km
	resolution	(~3–7 km) ~2–6 km	~3–4 km	~ 1 km	1.5–2.5 km	~2–4 km	~1–2 km	~2–5 km	–	~1–4 km
	utilized microwindows	831–853 cm^{-1}	mostly around 844 cm^{-1}	834 cm^{-1}	6.21–11.76 µm (1610–850 cm^{-1})	centered near 846 cm^{-1}	gas chromatography	840–860 cm^{-1}	gas chromatography	842.5–848.0 cm^{-1}
CFC-12	coverage	~5–40 km	~5–33 km	~8–33 km	10–35 km	~5–38 km	~10–35 km	~10–40 km	surface	~5–20 km
	resoulution	(~3–4 up to 8 km) slightly better	~3–4 km	~ 1 km	1.5–2.5 km	~2–4 km	~1–2 km	~2–5 km	–	~1–4 km
	utilized microwindows	915–925 cm^{-1}	922 cm^{-1}	915–932 cm^{-1}	6.21–11.76 µm (1610–850 cm^{-1})	922–1161 cm^{-1}	gas chromatography	918–924 cm^{-1}	gas chromatography	918.9–920.6 and 921.0–922.8 cm^{-1}

AMTD
8, 7573–7662, 2015

Table 2. Mean matching distance and time for comparisons based on collocated measurements.

Envisat/ MIPAS data set	MIPAS-STR	Aura/ HIRDLS	SCISAT/ ACE-FTS	ILAS-II
CFC-11 FR-period	–	–	355.62 km – 6.24 h	364.50 km – 3.25 h
CFC-12 FR-period	–	–	327.81 km – 5.59 h	364.88 km – 3.25 h
CFC-11 RR-period	171.78 km – 1.76 h	199.47 km – 2.89 h	375.77 km – 5.84 h	–
CFC-12 RR-period	171.78 km – 1.76 h	199.46 km – 2.89 h	378.78 km – 5.99 h	–

AMTD
8, 7573–7662, 2015

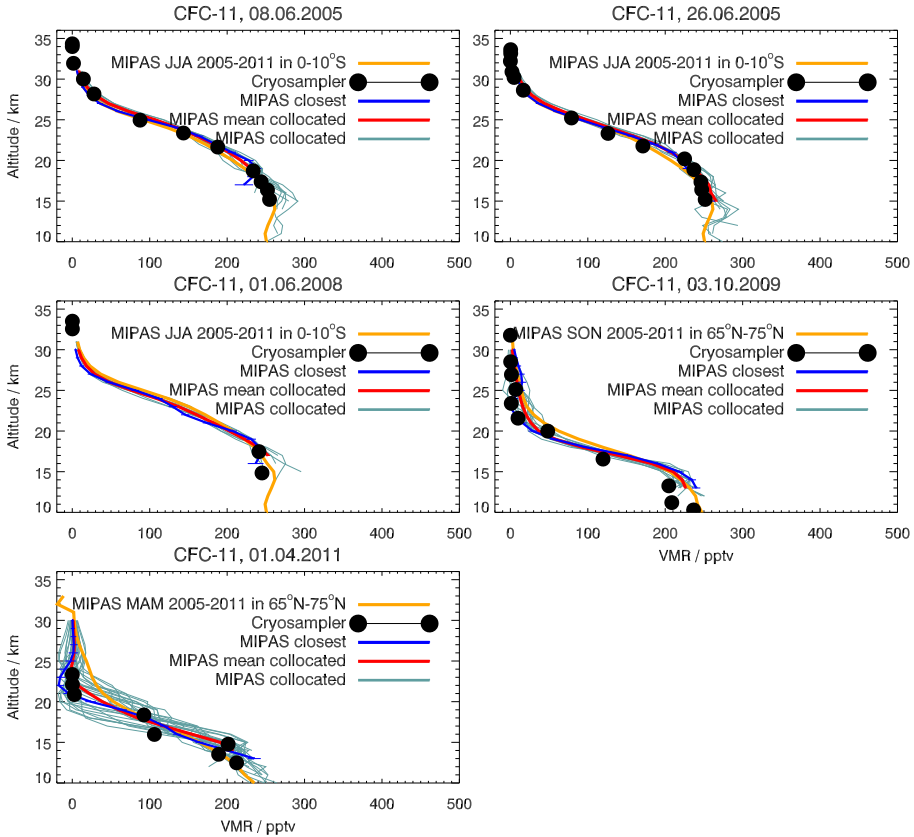

Figure 1. Comparison of a climatological mean of MIPAS Envisat CFC-11 measurements (light orange line), collocated measurements (blue-greyish lines) and their mean profile (red line) and the closest MIPAS Envisat profile (blue line) with different flights of Cryosampler (black dots).

AMTD
8, 7573–7662, 2015

MIPAS IMK/IAA CFC-11 and CFC-12: accuracy, precision and long-term stability

E. Eckert et al.

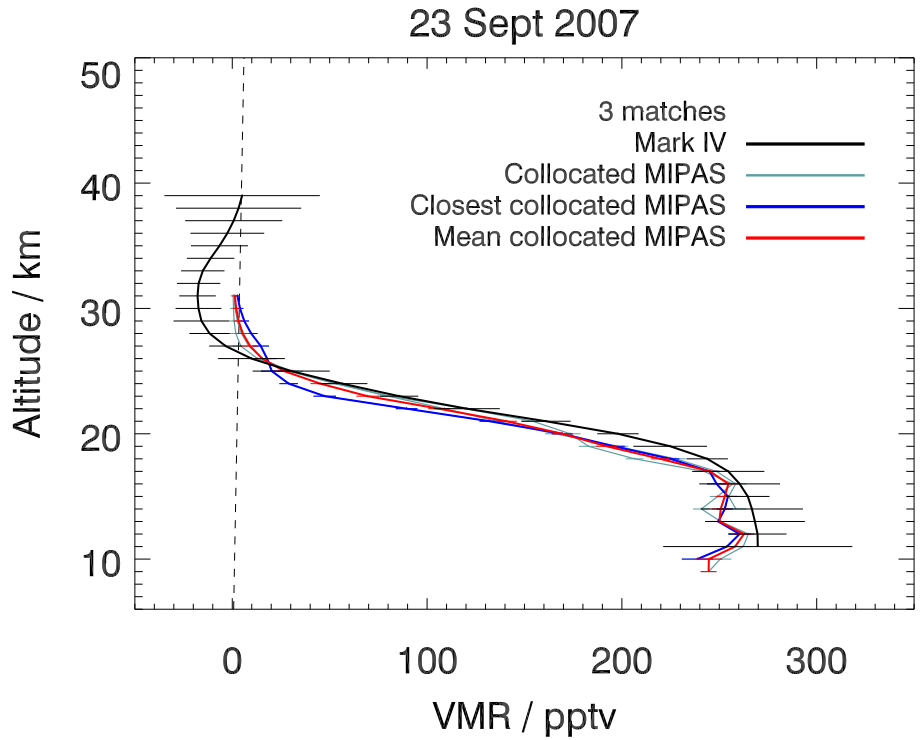

Figure 2. Comparison of one MkIV CFC-11 profile (black line) with three coincident profiles of MIPAS Envisat (blue-greyish lines). The closest (blue line) and the mean (red line) of these profiles (blue line) are shown in addition. The MkIV error estimates are inferred from the fit residuals.

AMTD
8, 7573–7662, 2015

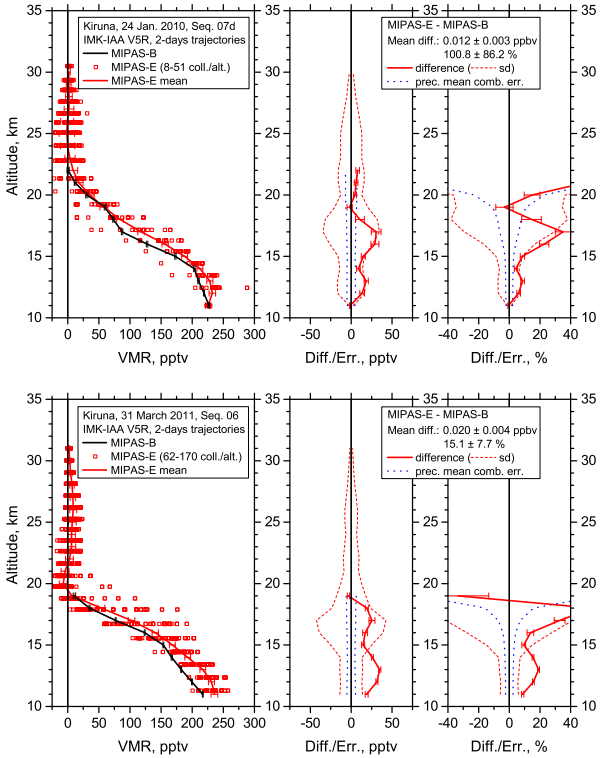

Figure 3. Comparison of a mean profile of MIPAS Envisat CFC-11 collocated measurements (left panels: red line) with a profile of MIPAS-B (black line) obtained on 24 January 2010 (upper panels) and 31 March 2011 (lower panels) at Kiruna. The error bars (1σ; left panel) show the retrieval noise for MIPAS Envisat and MIPAS-B. The difference is shown in absolute (middle panels) and relative (right panels) terms. The dotted red line is the standard deviation and dotted blue line is the combined error which consists of the root of the squared error of MIPAS-B and the MIPAS Envisat mean.

AMTD
8, 7573–7662, 2015

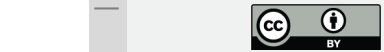

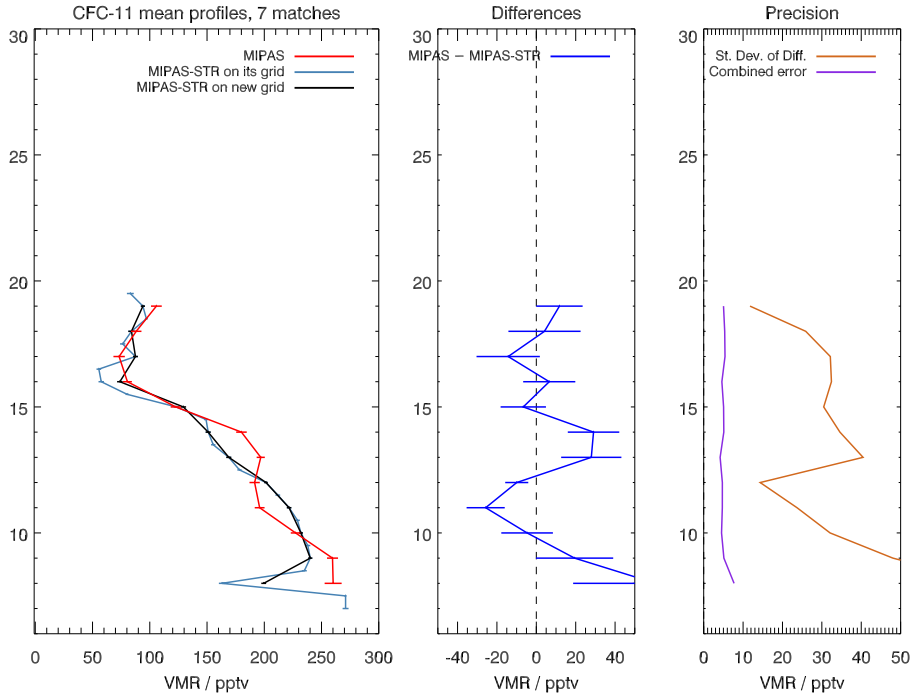

Figure 4. Comparison of mean profiles of MIPAS Envisat CFC-11 (left panel, red line) and MIPAS-STR (left panel, black line) for 7 collocated measurements taken during a flight in March 2011. The error bars consist of the retrieval noise for both MIPAS Envisat and MIPAS-STR. The middle panel shows the mean difference (blue) of these profiles and the standard error of the mean. The right panel shows the combined error (purple) of the instruments and the standard deviation of the differences (brown).

AMTD
8, 7573–7662, 2015

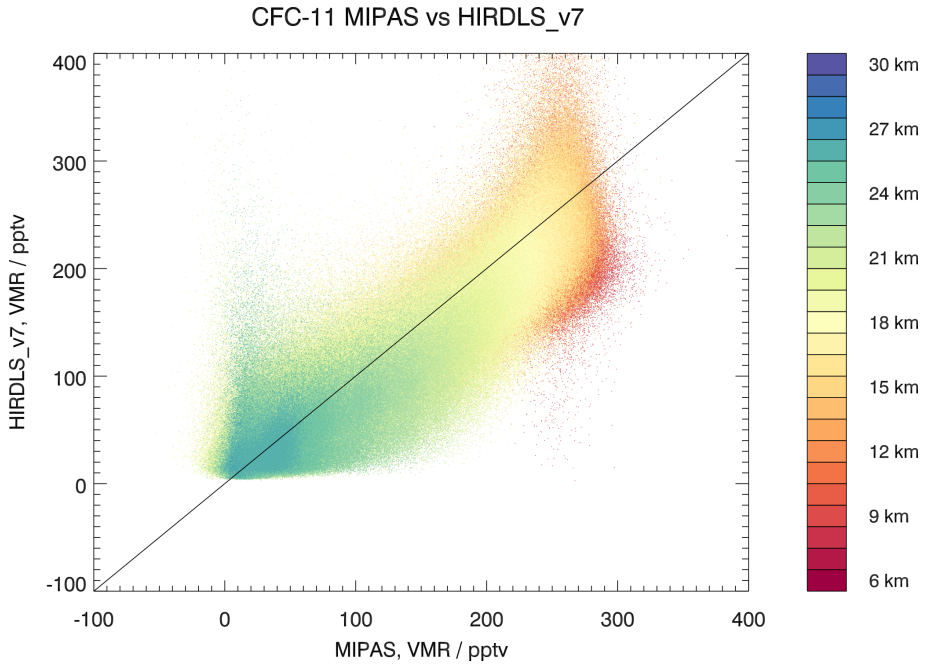

Figure 5. Correlation of collocated MIPAS Envisat CFC-11 measurements with HIRDLS measurements during the time period of 2005–2008.

AMTD
8, 7573–7662, 2015

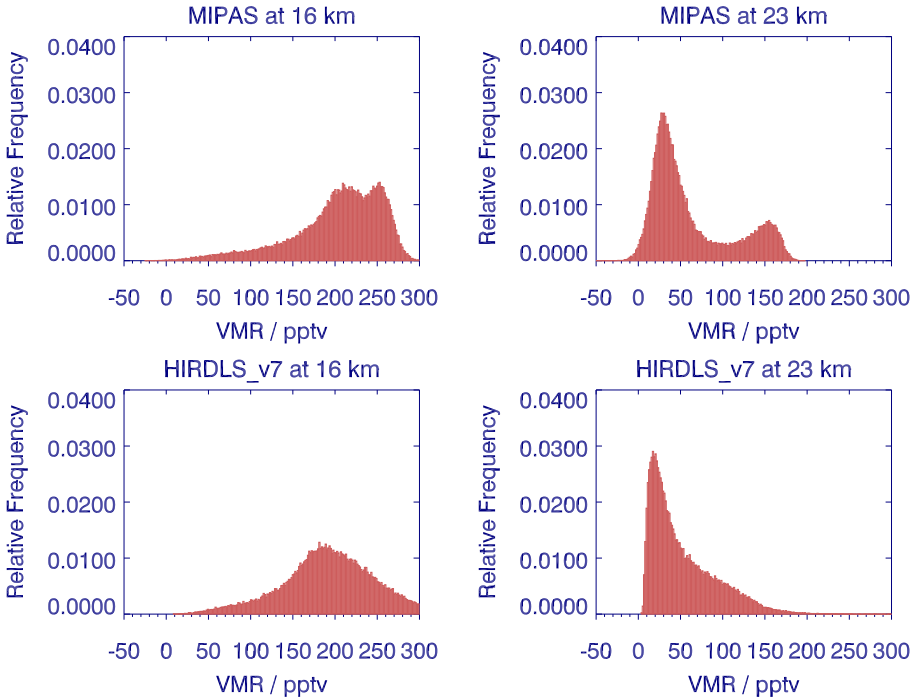

Figure 6. Histogram of collocated MIPAS Envisat CFC-11 measurements (top panels) and HIRDLS measurements (bottom panels) for the years of 2005–2008 at 16 km (left panels) and 23 km (right panels).

AMTD
8, 7573–7662, 2015

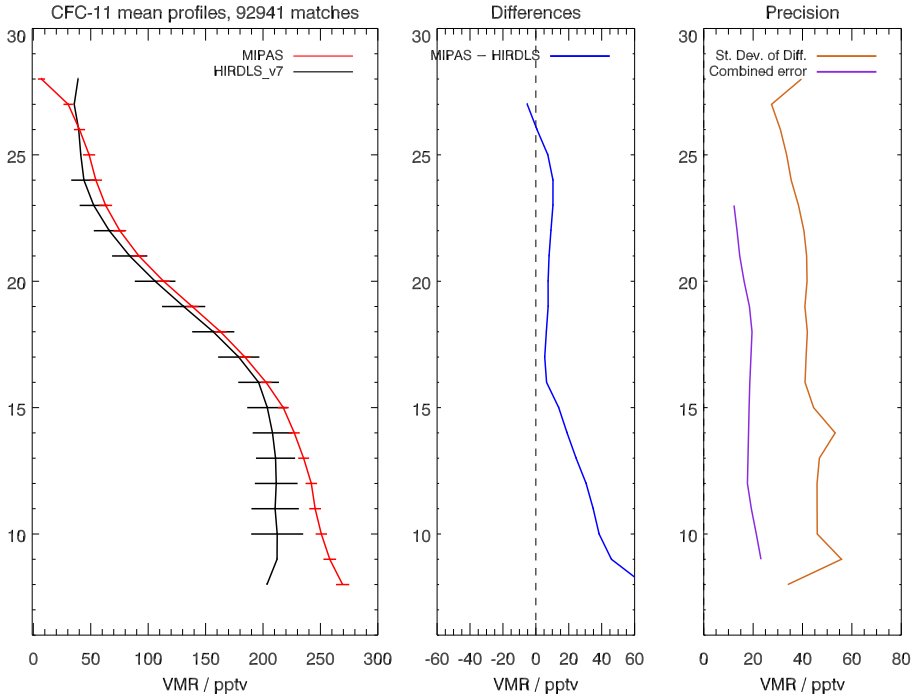

Figure 7. Comparison of mean profiles of MIPAS Envisat CFC-11 (left panel, red line) and HIRDLS (left panel, black line) for the years of 2005–2008. The error bars include the retrieval noise in the case of MIPAS and the estimated error – which is derived from the average of 10 sets of 12 consecutive profiles of regions with little variability (Gille et al., 2014) – in the case of HIRDLS. The middle panel shows the mean difference (blue) of these profiles and the standard error of the mean. The middle and right panel show the same components as in Fig. 4.

AMTD
8, 7573–7662, 2015

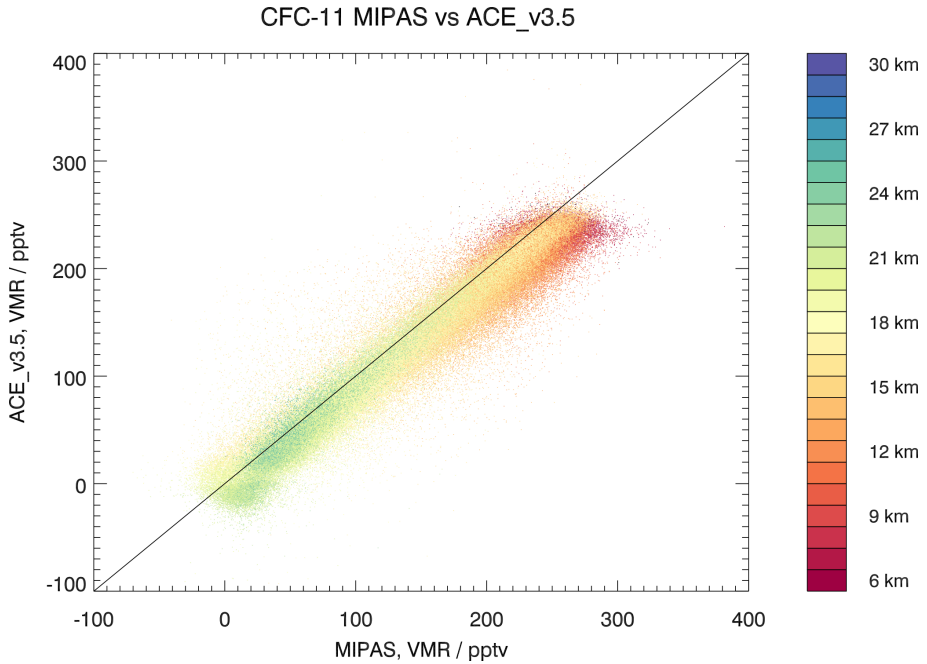

Figure 8. Correlation of collocated MIPAS Envisat CFC-11 measurements with ACE-FTS measurements during the time period of 2005–2012.

AMTD
8, 7573–7662, 2015

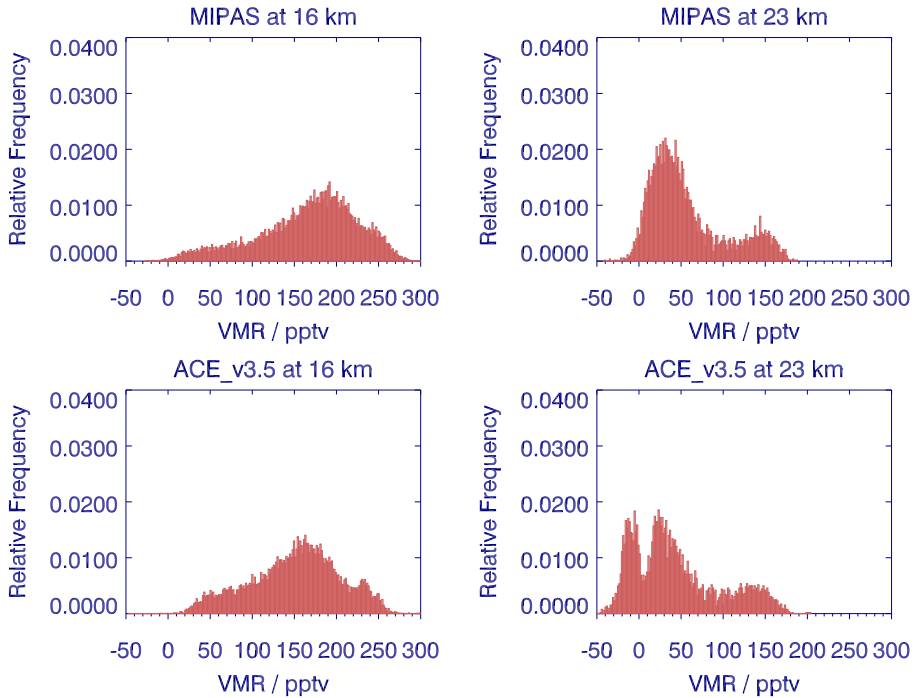

Figure 9. Histogram of MIPAS Envisat CFC-11 measurements (top panels) and ACE-FTS measurements (bottom panels) for the years 2005–2012 at 16 km (left panels) and 23 km (right panels).

AMTD
8, 7573–7662, 2015

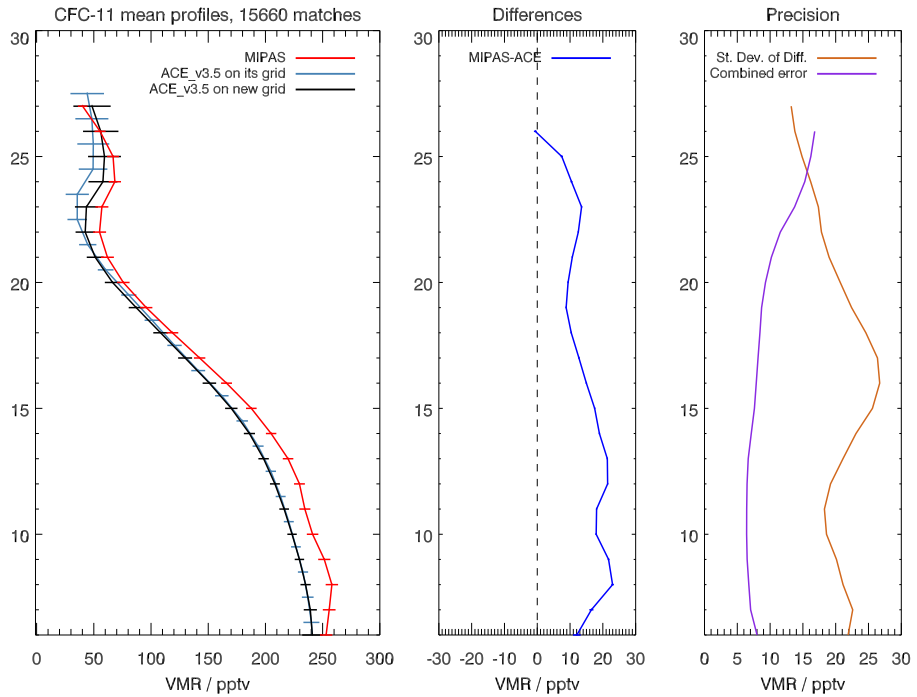

Figure 10. Comparison of mean profiles of MIPAS Envisat CFC-11 (left panel, red line) and ACE-FTS (left panel: steel blue line = ACE-FTS on native grid; black line = ACE-FTS interpolated onto the MIPAS Envisat grid) for the years of 2005–2012. The error bars include the retrieval noise in the case of both instruments. The middle and right panel show the same components as in Fig. 4.

AMTD
8, 7573–7662, 2015

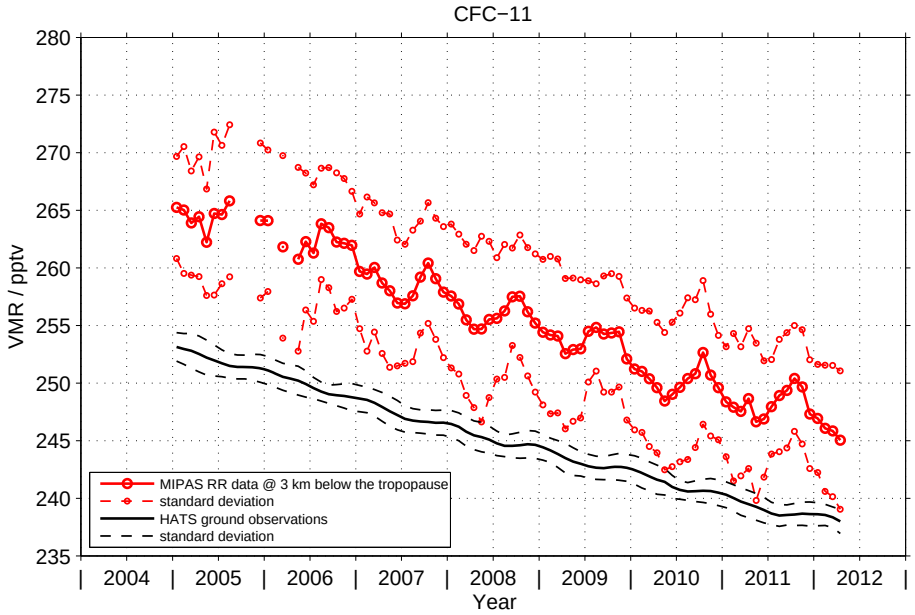

Figure 11. Comparison of MIPAS Envisat CFC-11 values at 3 km below the tropopause (red) and ground based measurements of the HATS network (black). Dashed lines denote the standard deviation.

AMTD
8, 7573–7662, 2015

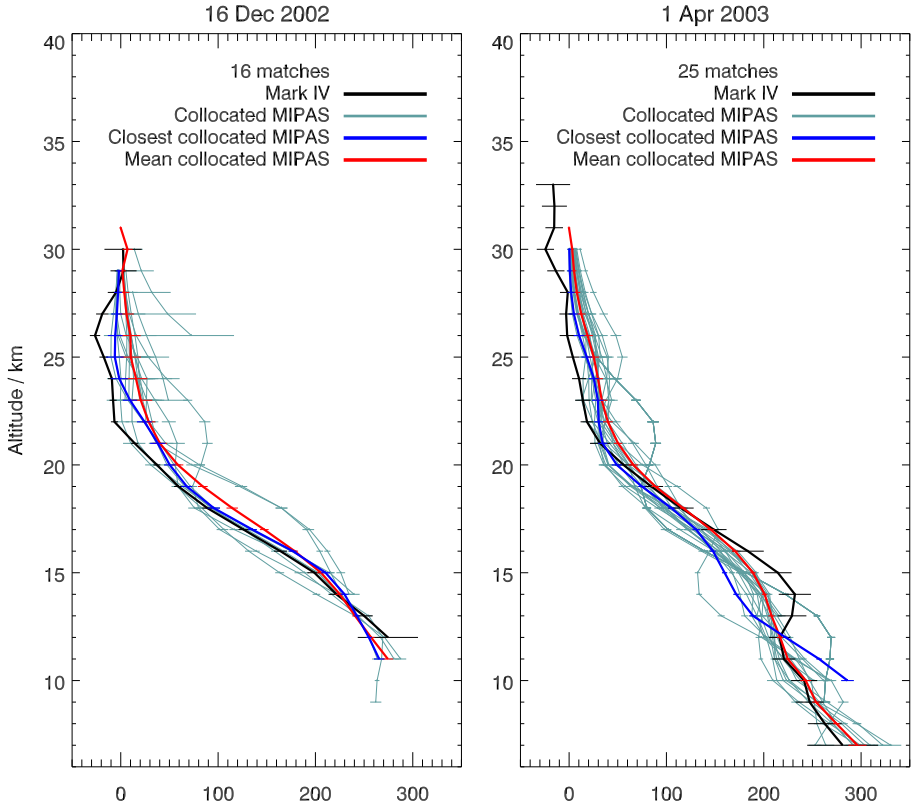

Figure 12. Two MkIV profiles are compared with collocated MIPAS Envisat of the FR period. For the measurement on 16 December 2002, 16 collocated MIPAS Envisat measurements were found, while 25 MIPAS Envisat profiles coincided with the 1 April 2003 MkIV measurement. The setup is similar to Fig. 2.

AMTD
8, 7573–7662, 2015

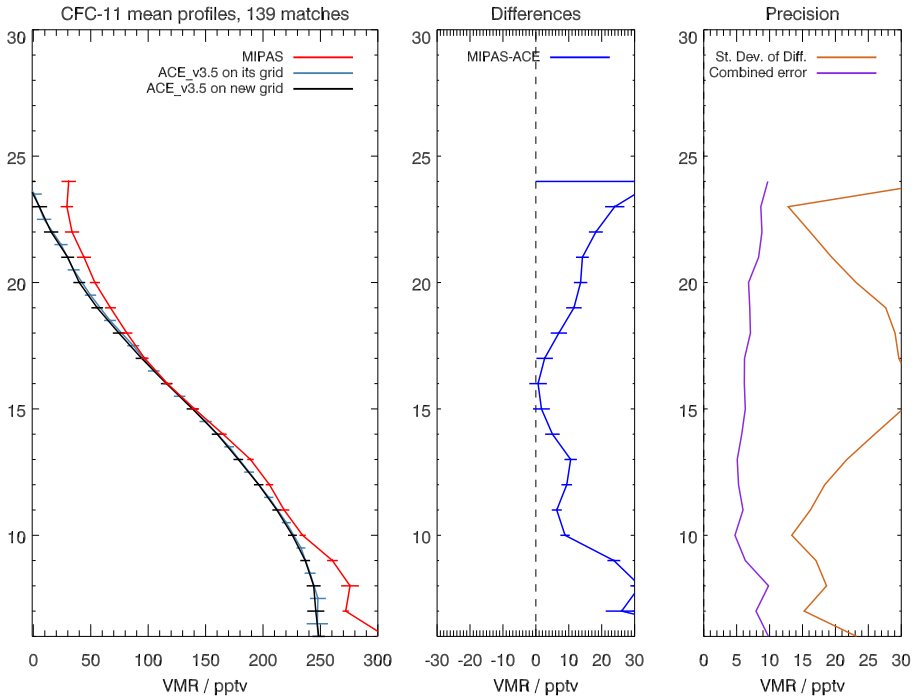

Figure 13. Same as in Fig. 10, but for the MIPAS Envisat FR time period data set (V5H_CFC-11_20).

AMTD
8, 7573–7662, 2015

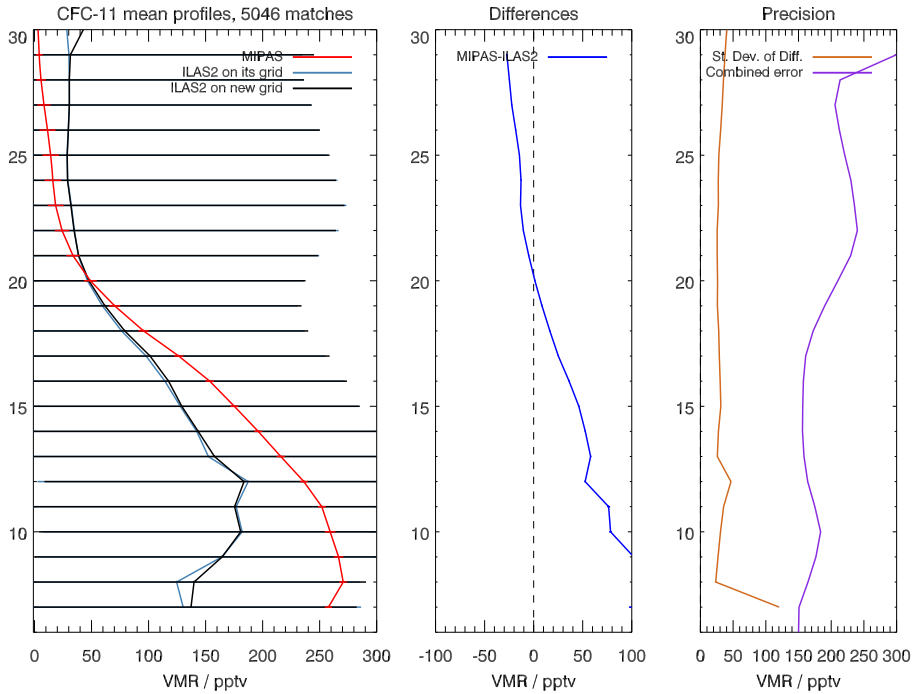

Figure 14. Same as in Fig. 13, but for the comparison of ILAS-II with MIPAS Envisat.

AMTD
8, 7573–7662, 2015

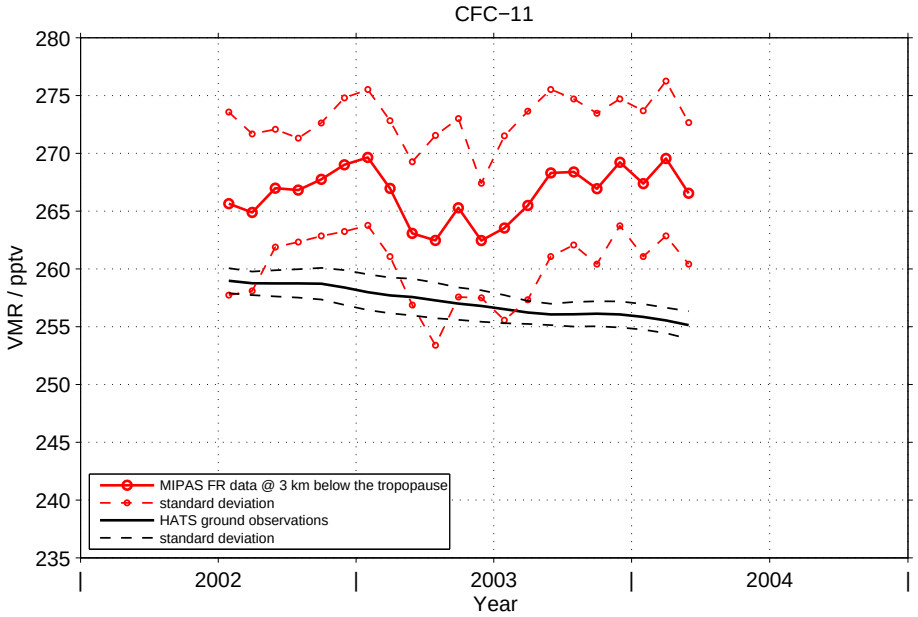

Figure 15. Same as in Fig. 11, but for the MIPAS Envisat FR time period data set (V5H_CFC-11_20).

AMTD
8, 7573–7662, 2015

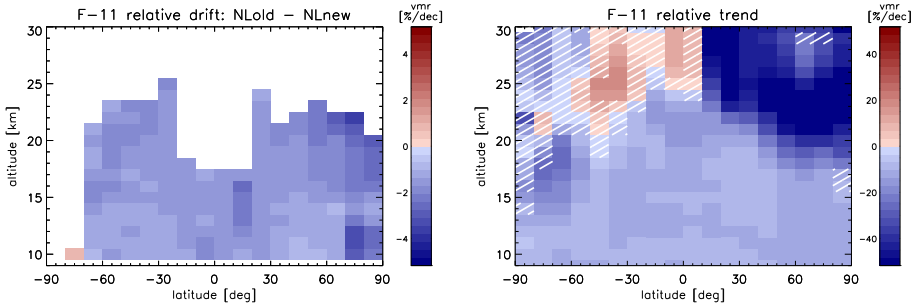

Figure 16. Left panel: altitude–latitude cross-section of the instrument drift in MIPAS CFC-11. This drift is calculated by comparing the temporal evolution the CFC-11 from two different setups. One setup uses non-linearity correction coefficient used for the bulk MIPAS retrieval to date. The other uses newly suggested time-dependent non-linearity correction coefficients (comp. Eckert et al., 2014, Sect. 3.3). The drift is shown in relative terms, referring to the mean CFC-11 mixing ratio in the middle of the time series. Blueish tiles indicate that the new coefficients result in higher CFC-11 mixing ratios, while reddish tiles indicate the opposite. White areas indicate that there were too few or no data points available to estimate a drift properly. Right panel: altitude–latitude cross-section of relative MIPAS Envisat CFC-11 trends, calculated from data covering January 2005–April 2012. The trend is weighted with the CFC-11 mixing ratio of the middle of the time series for each tile. Blueish tiles indicate declining CFC-11 mixing ratios, while increasing mixing ratios are represented by reddish tiles. Hatching indicates that the trends are either not significant at 2-sigma level or that χ^2 is more than 10 % different from one.

AMTD
8, 7573–7662, 2015

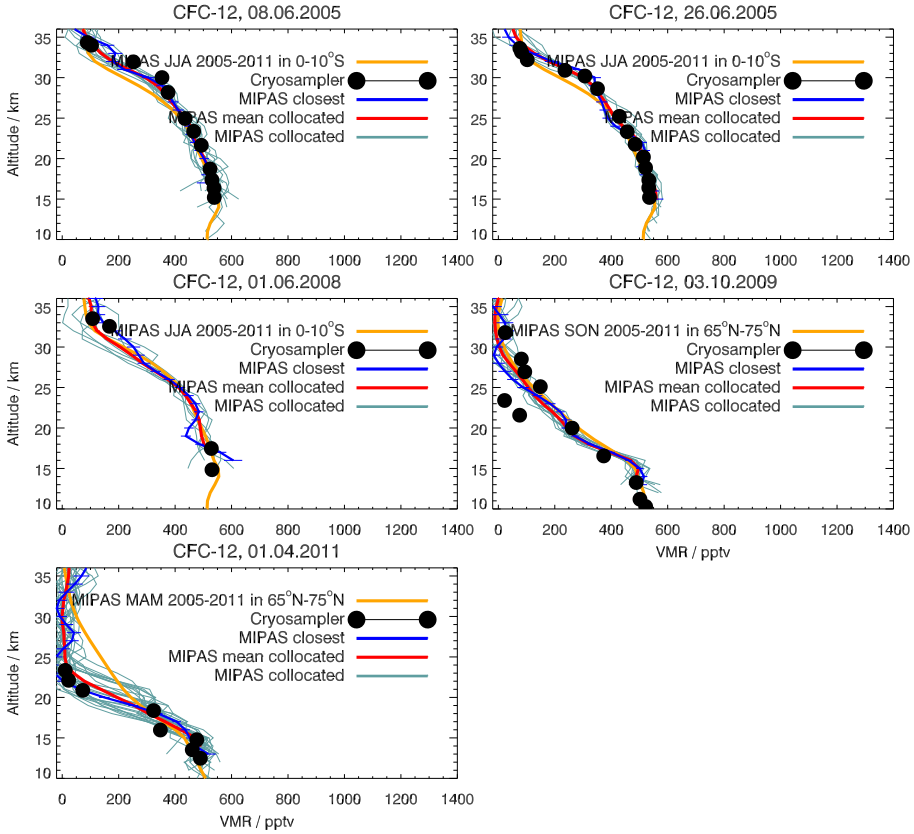

Figure 17. Comparison of an ensemble of MIPAS Envisat CFC-12 measurements (light orange lines), collocated measurements (blue-greyish lines) and their mean profile (red line) and the closest MIPAS Envisat profile (blue line) with different flights of Cryosampler (black dots).

AMTD
8, 7573–7662, 2015

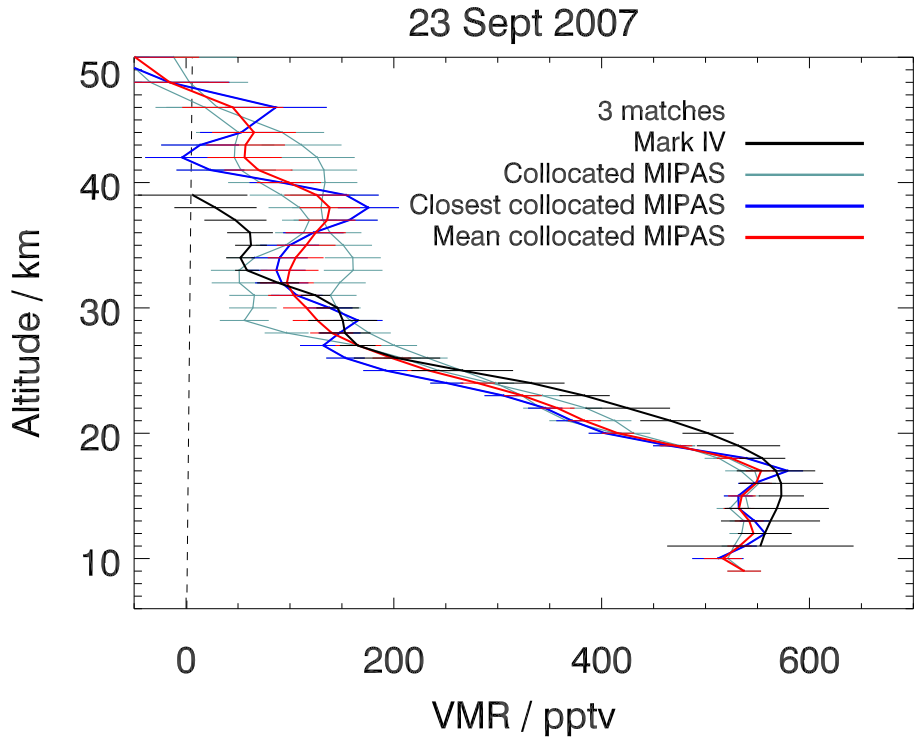

Figure 18. Same as in Fig. 2, but for CFC-12.

AMTD
8, 7573–7662, 2015

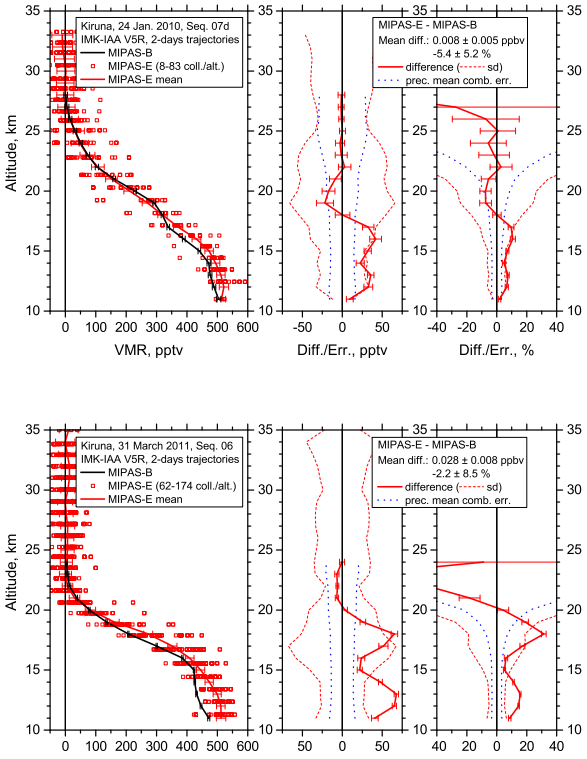

Figure 19. Same as in Fig. 3 but for CFC-12.

AMTD
8, 7573–7662, 2015

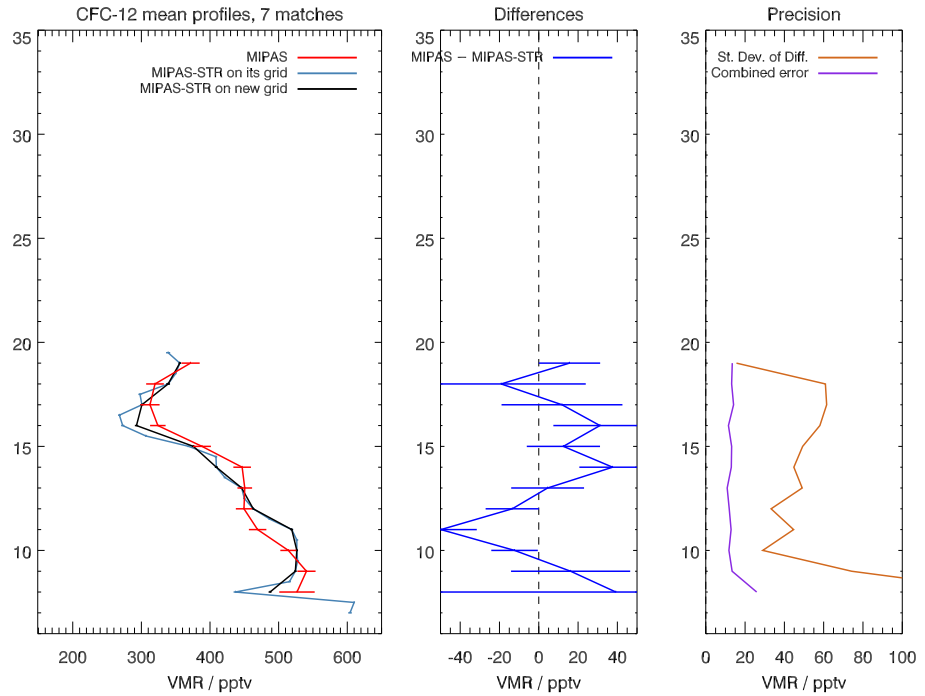

Figure 20. Same as in Fig. 4 but for CFC-12.

AMTD
8, 7573–7662, 2015

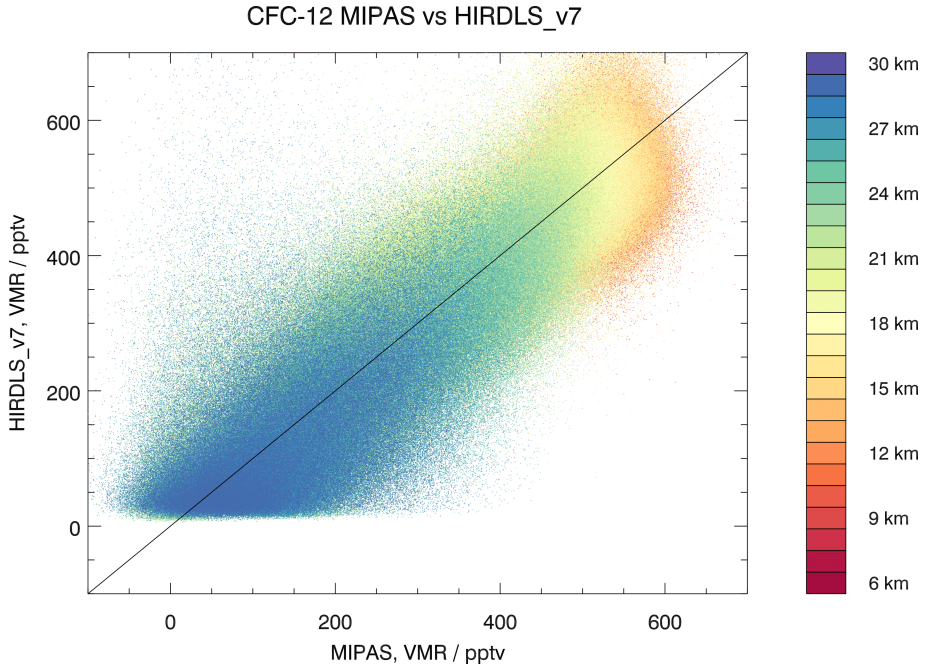

Figure 21. Correlation of collocated MIPAS Envisat CFC-12 measurements with HIRDLS measurements during the time period of 2005–2008.

AMTD
8, 7573–7662, 2015

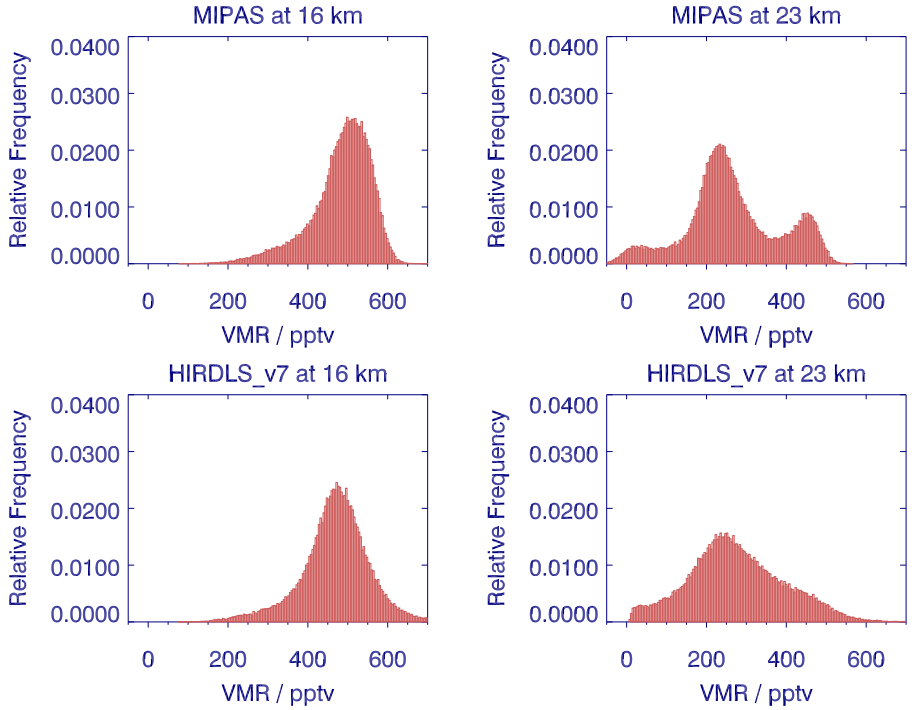

Figure 22. Histogram of collocated MIPAS Envisat CFC-12 measurements (top panels) and HIRDLS measurements (bottom panels) for the years of 2005–2008 at 16 km (left panels) and 23 km (right panels).

AMTD
8, 7573–7662, 2015

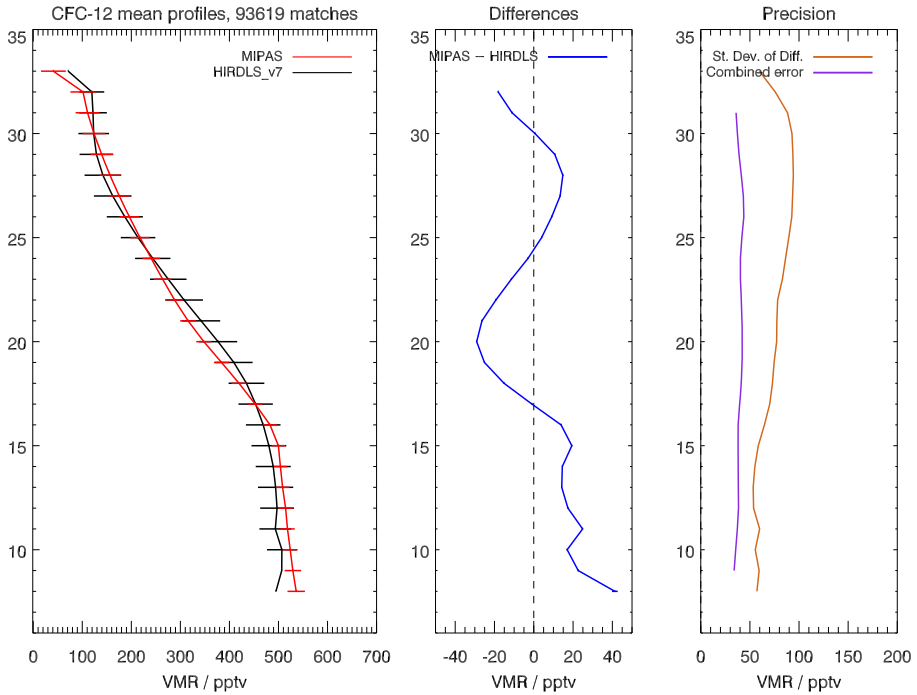

Figure 23. Same as in Fig. 7 but for CFC-12.

AMTD
8, 7573–7662, 2015

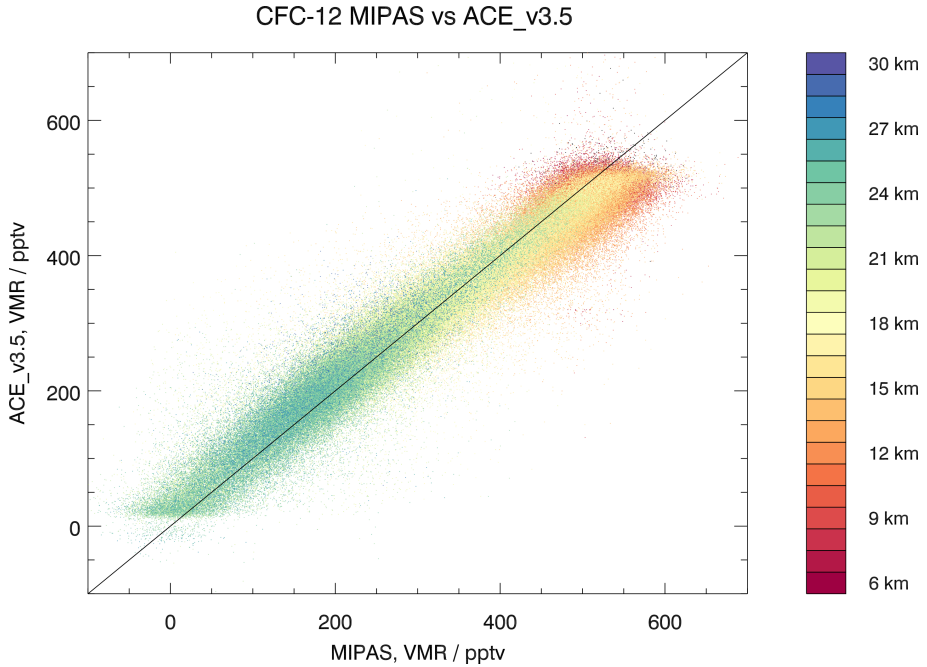

Figure 24. Correlation of collocated MIPAS Envisat CFC-12 measurements with ACE-FTS measurements during the time period of 2005–2012.

AMTD
8, 7573–7662, 2015

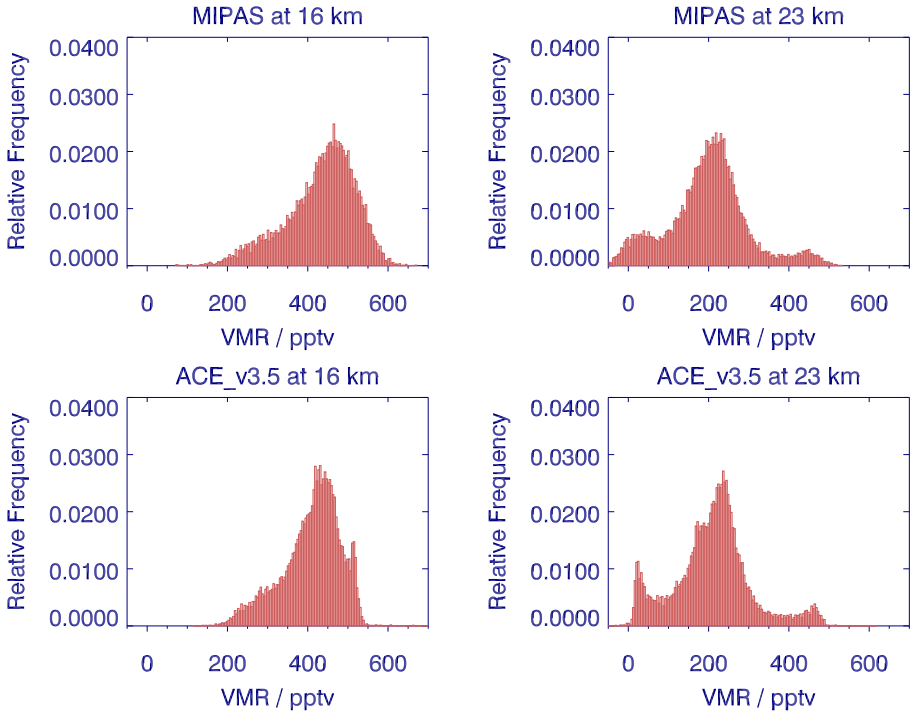

Figure 25. Histogram of MIPAS Envisat CFC-12 measurements (top panels) and ACE-FTS measurements (bottom panels) for the years of 2005–2012 at 16 km (left panels) and 23 km (right panels).

AMTD
8, 7573–7662, 2015

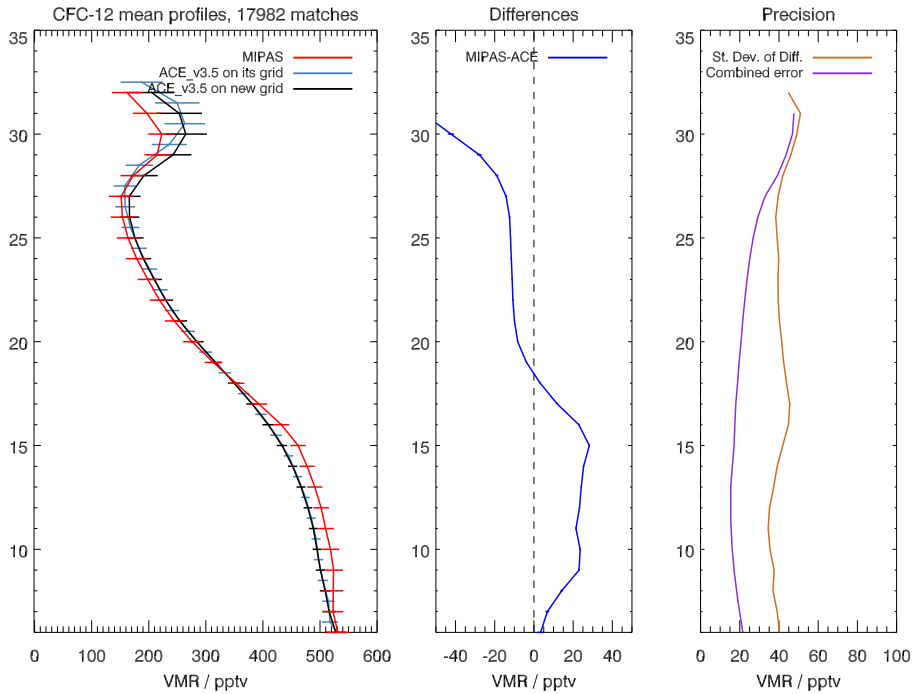

Figure 26. Same as in Fig. 10 but for CFC-12.

AMTD
8, 7573–7662, 2015

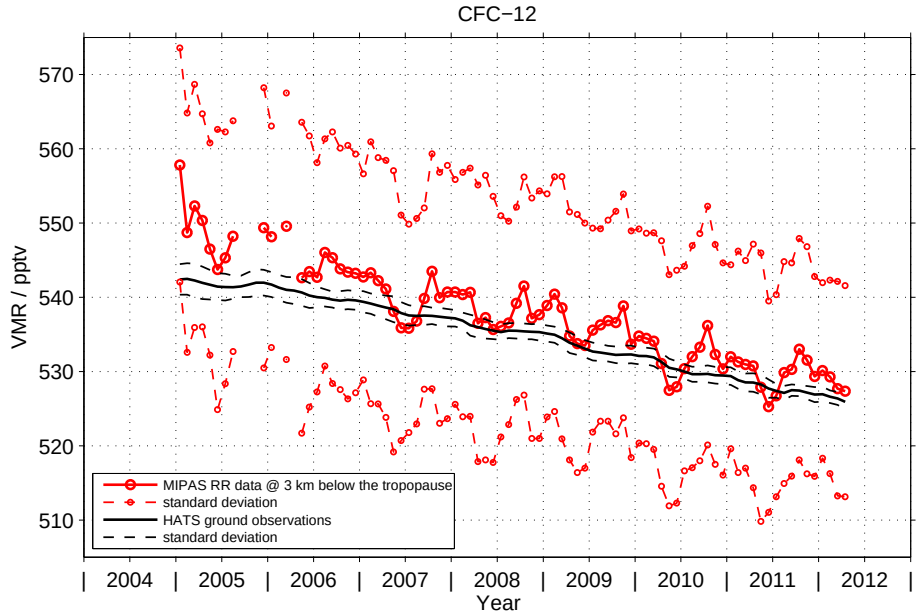

Figure 27. Comparison of MIPAS Envisat CFC-12 value estimates at 3 km below the tropopause (red) and ground based measurements collected by the HATS network (black).

AMTD
8, 7573–7662, 2015

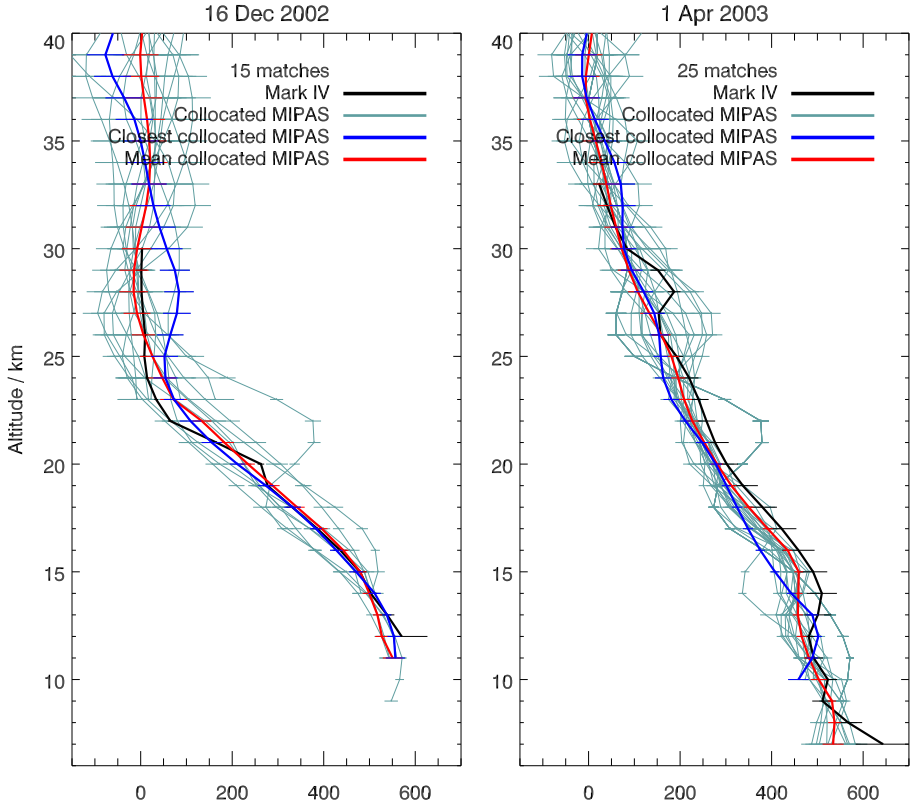

Figure 28. Similar to Fig. 12, but for CFC-12.

AMTD
8, 7573–7662, 2015

MIPAS IMK/IAA CFC-11 and CFC-12: accuracy, precision and long-term stability

E. Eckert et al.

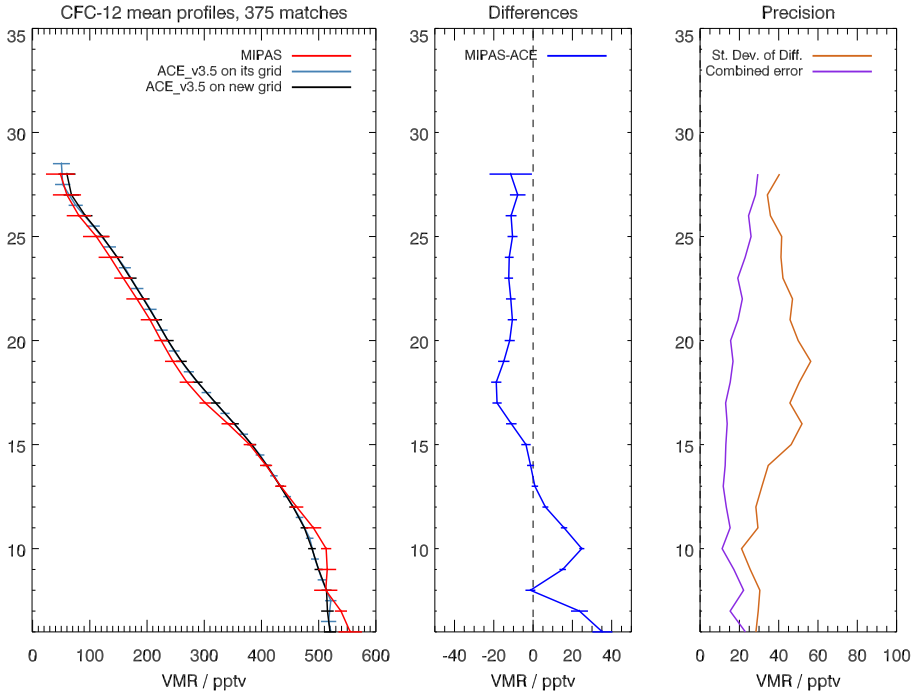

Figure 29. Same as in Fig. 26, but for the MIPAS Envisat FR time period data set (V5H_CFC-12_20).

AMTD
8, 7573–7662, 2015

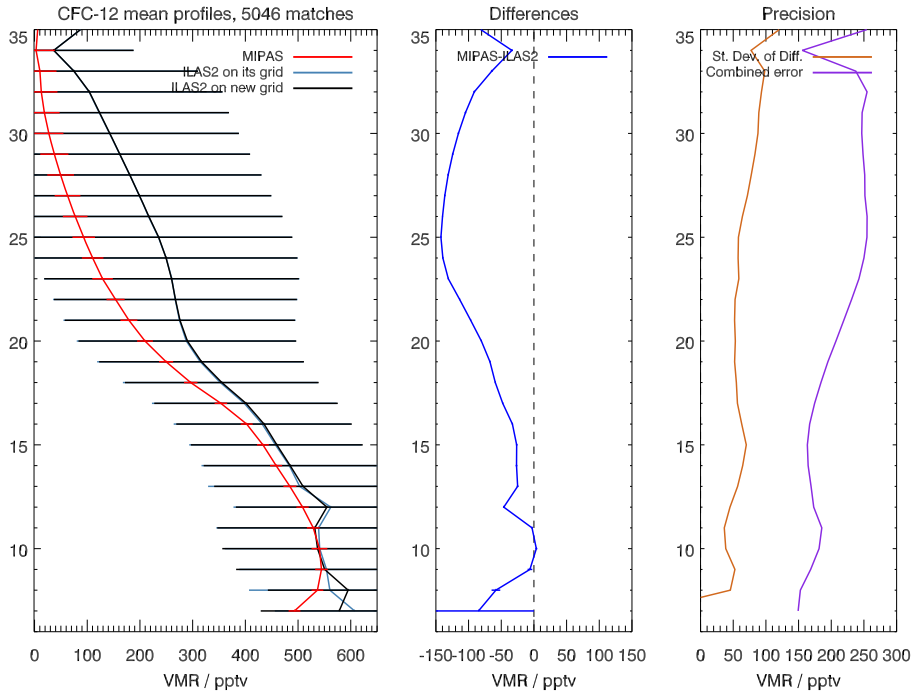

Figure 30. Same as in Fig. 14, but for CFC-12.

AMTD
8, 7573–7662, 2015

MIPAS IMK/IAA CFC-11 and CFC-12: accuracy, precision and long-term stability

E. Eckert et al.

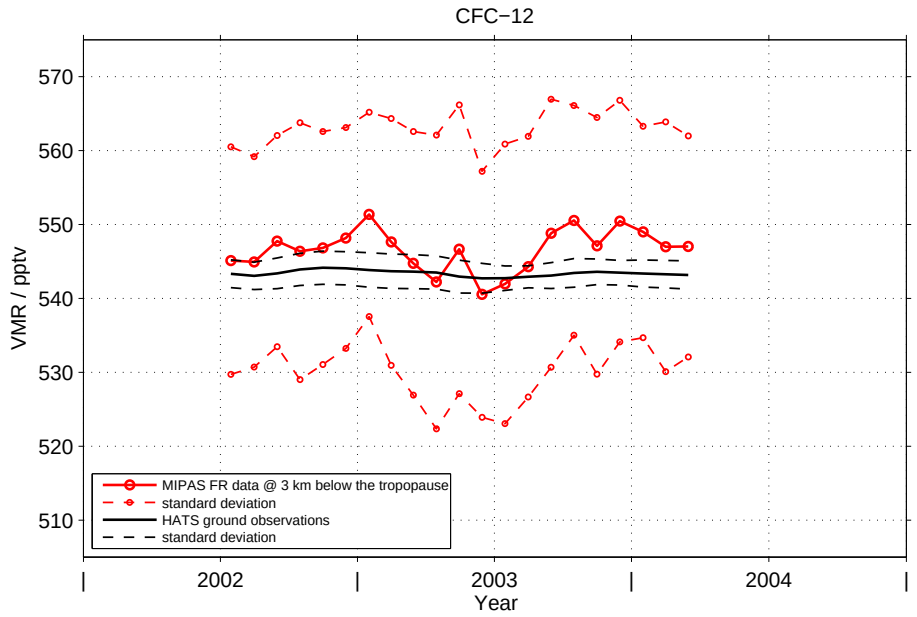

Figure 31. Same as in Fig. 27, but for the MIPAS Envisat FR time period data set (V5H_CFC-12_20).

AMTD
8, 7573–7662, 2015

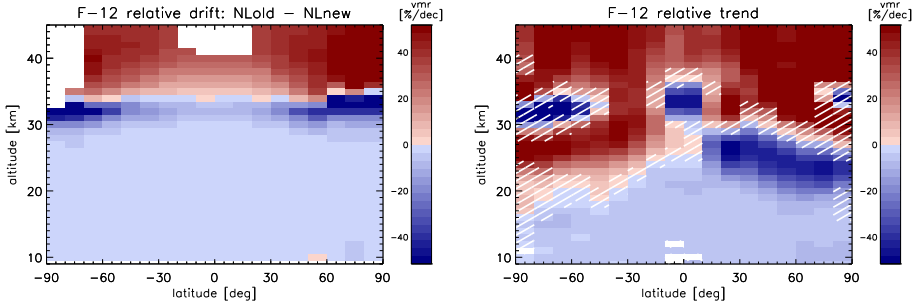

Figure 32. Same as in Fig. 16 but for CFC-12.

AMTD
8, 7573–7662, 2015

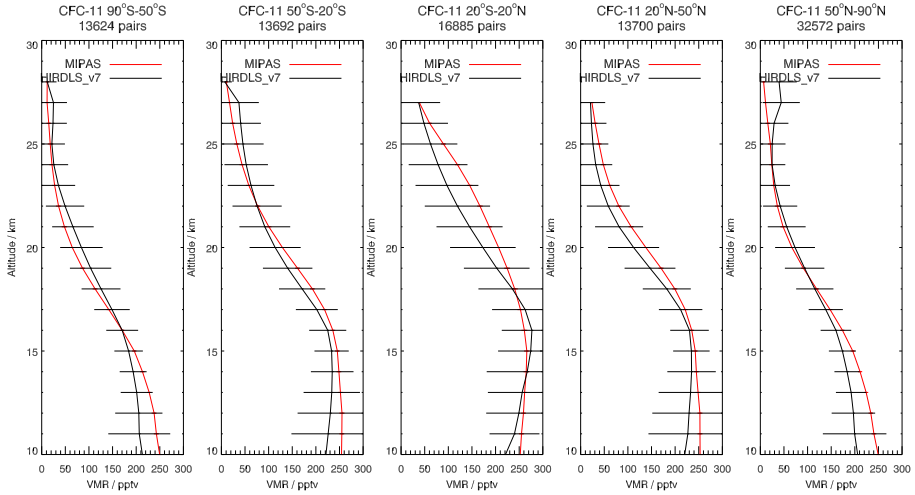

Figure A1. Comparison of mean profiles of MIPAS Envisat CFC-11 (red line) and HIRDLS (black line) for different latitude bins for the years of 2005–2008. The error bars include the retrieval noise in the case of both instruments.

AMTD
8, 7573–7662, 2015

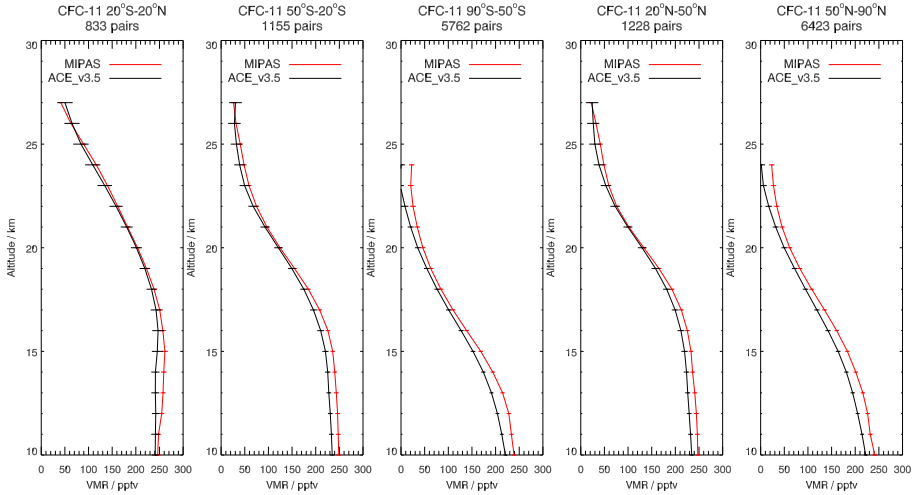

Figure A2. Comparison of mean profiles of MIPAS Envisat CFC-11 (red line) and ACE-FTS (black line) for different latitude bins for the years of 2005–2012. The error bars include the retrieval noise in the case of both instruments.

AMTD
8, 7573–7662, 2015

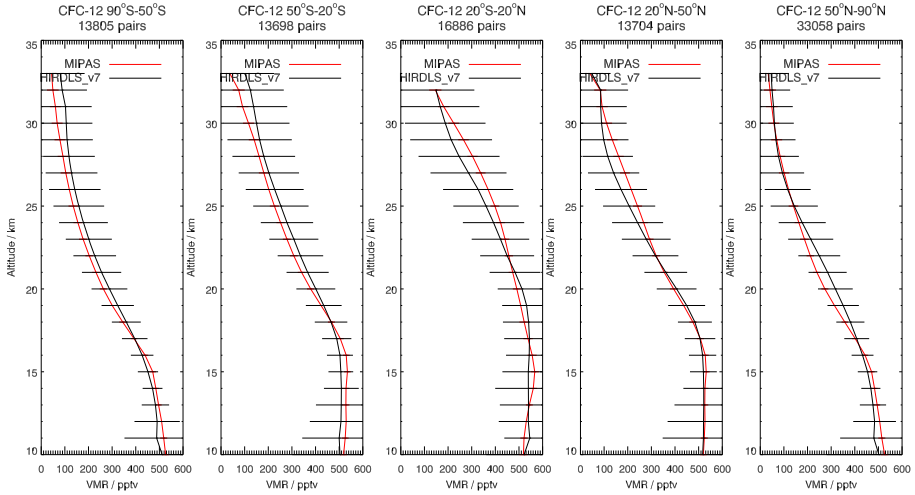

Figure A3. Comparison of mean profiles of MIPAS Envisat CFC-12 (red line) and HIRDLS (black line) for different latitude bins for the years of 2005–2008. The error bars include the retrieval noise in the case of both instruments.

AMTD
8, 7573–7662, 2015

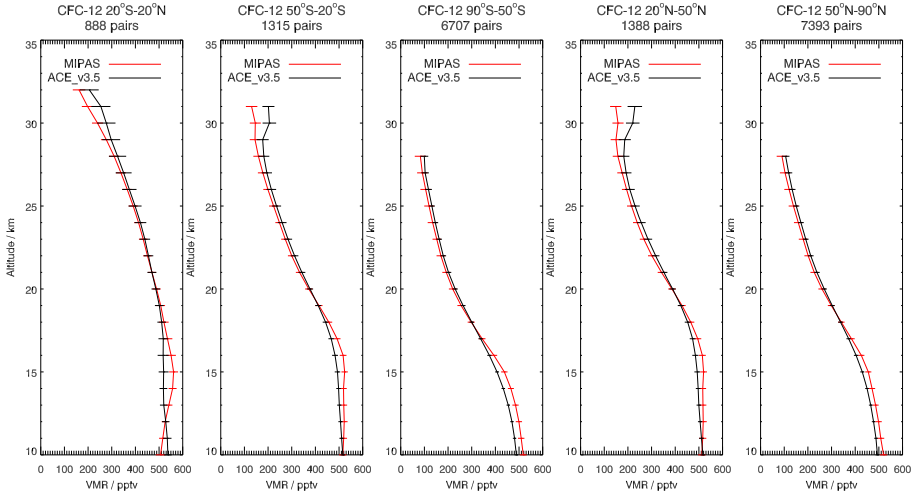

Figure A4. Comparison of mean profiles of MIPAS Envisat CFC-12 (red line) and ACE-FTS (black line) for different latitude bins for the years of 2005–2012. The error bars include the retrieval noise in the case of both instruments.

AMTD
8, 7573–7662, 2015